https://doi.org/10.5194/tc-2019-280
Preprint. Discussion started: 7 January 2020

The Cryosphere Discussions
Open Access
EGU

Estimating fractional snow cover from passive microwave brightness temperature data using MODIS snow cover product over North America

Xiongxin Xiao[1], Shunlin Liang[2], Tao He[1], Daiqiang Wu[1], Congyuan Pei[1], Jianya Gong[1]

[1] School of Remote Sensing and Information Engineering, Wuhan University, Wuhan 430079, China

[2] Department of Geographical Sciences, University of Maryland, College Park, MD 20742, USA

Correspondence to: Tao He (taohers@whu.edu.cn)

Abstract: The dynamic characteristics of seasonal snow cover are critical for hydrology management, climate system, and ecosystem function. Although optical satellite remote sensing has proved to be an effective tool for monitoring global and regional variations of snow cover, it is still problematic to accurately capture the snow dynamics characteristics at a finer spatiotemporal resolution, because the observations from optical satellite sensors are seriously affected by clouds and solar illumination. Besides, traditional methods of mapping snow cover from passive microwave data only provide binary information with a 25-km spatial resolution. In this study, we first present an approach to predict fractional snow cover over North America under all-weather conditions, derived from the enhanced resolution passive microwave brightness temperature data (6.25 km). This estimation algorithm used Moderate Resolution Imaging Spectroradiometer (MODIS) snow cover products between 2010 and 2017 to create the reference fractional snow cover data as the "true" observations. Further, the influence of many factors, including land cover, topography, and location, were incorporated into the retrieval models. The results show that the proposed retrieval models based on random forest regression technique perform much better using independent test data for all land cover classes, with higher accuracy and no out-of-range estimated values, when compared to the other three approaches (linear regression, artificial neural networks (ANN), and multivariate adaptive regression splines (MARS)). The results of the output evaluated by using independent data from 2017 indicate that the root-mean-square error (RMSE) of the estimated fractional snow cover ranges from 16.7% to 19.8%. In addition, the estimated fractional snow cover is verified in the snow mapping aspect by using snow cover observation data from meteorological stations (more than 0.31 million records). The result shows that the binary snow cover obtained by the proposed retrieval algorithm is in a good agreement with the ground measurements (kappa: 0.67). The accuracy of our algorithm estimation in the snow cover identification shows significant improvement when benchmarked against the Grody's snow cover mapping algorithm: overall accuracy is increased by 18% (from 0.71 to 0.84), and omission error is reduced by 71% (from 0.48 to 0.14). According to our experiment results, we can conclude that it is feasible for estimating fractional snow cover from passive microwave brightness temperature data, and this strategy also has a great advantage in detecting snow cover area.

https://doi.org/10.5194/tc-2019-280
Preprint. Discussion started: 7 January 2020

1. Introduction

Snow cover is a critical indicator of climate change and plays a vital role in the global energy budget (Flanner et al., 2011), water cycles (Gao et al., 2019), and atmospheric circulation (Henderson et al., 2018). Snow cover directly modulates the release of carbon and methane from the underlying soil (Zhang, 2005; Zona et al., 2016), and influences the permafrost conditions and active layer dynamics (Zona et al., 2016). Moreover, snowpack stores a vast number of water resources providing water for both domestic and industrial use (Sturm, 2015; Cheng et al., 2019). Accurate and timely monitoring of snow cover spatiotemporal variation is beneficial for hydrologic forecast, climate prediction and water resources management (Barnett et al., 2005; Bormann et al., 2018).

Usually, snow cover data is obtained from meteorological stations or in-situ measurements, which are time-consuming, cumbersome, and spatially discontinuous. Remote sensing can cover a wide area and is capable of high frequency observations; therefore, it has been an attractive alternative tool to ground-based measurements. Numerous studies focused on snow cover detection and snow cover products used optical and microwave satellite data (Tsai et al., 2019; Liu et al., 2018; Hori et al., 2017). Most of these snow cover products provide binary information at pixel-level, either snow-covered or snow-free. However, snow cover often varies within a limited scale area, showing high spatial heterogeneity, especially in alpine terrain areas. Dobreva and Klein (2011) demonstrated that the use of binary snow cover classification in snow cover area estimation could produce considerable uncertainties. The binary snow cover lacking fractional feature hinders the capabilities of accurately characterizing the spatial distribution of snow cover and cannot accurately captures the season snow cover dynamic variations. From the energy budget perspective, binary snow cover will bring significant uncertainties into the global energy budget estimation due to huge difference in surface albedo between snow-covered and snow-free surfaces (He et al., 2014). Thus, snow cover area within a sub-pixel is urgently needed for providing accurate snow cover information. Therefore, focusing on fractional instead of binary snow cover is a better option, which means deriving the snow cover area at the sub-pixel level (Salomonson and Appel, 2004).

Fractional snow cover maps derived from optical imagery have been produced for over 40 years. It is generally well known that optical satellite observations are suitable for estimating fractional snow cover because of their high spatial resolution. Moderate to high resolution optical observations are popular in previous snow cover studies, for example FY series sensors (0.5 ~ 4 km) (Wang et al., 2017), Moderate Resolution Imaging Spectroradiometer (MODIS) (500 m) (Kuter et al., 2018), Landsat (30 m) (Berman et al., 2018). There are also many methods for predicting fractional snow cover, such as, linear regression (Salomonson and Appel, 2004; Salomonson and Appel, 2006); spectral mixture analysis (Wang et al., 2017; Rosenthal and Dozier, 1996); machine learning, e.g., artificial neural network (ANN) (Liang et al., 2017; Moosavi et al., 2014); and multivariate adaptive regression splines (MARS) (Kuter et al., 2018). A simple linear regression cannot fully describe the complexity of the relationship between satellite observations and fractional snow cover; thus, non-linear approaches were

https://doi.org/10.5194/tc-2019-280
Preprint. Discussion started: 7 January 2020

recently developed to replace this traditional method (Berman et al., 2018). Kuter et al. (2018) estimated fractional snow cover from MODIS data using the MARS technique, where the Landsat 8 binary snow cover data served as reference fractional snow cover data. The results indicated that the estimated fractional snow cover from MARS method is in good agreement with the reference fractional snow cover with average values of R = 0.93 (correlation coefficient) (Kuter et al., 2018). However, clouds and the limited solar illumination in polar regions have become the greatest challenges in snow cover detection from optical satellite data, resulting in snow cover maps with incomplete spatial coverage with gaps sometimes up to 70% (Parajka and Blöschl, 2008). Constant efforts have been made to fill the gaps mainly caused by cloud contamination by fusing multi-source data (Chen et al., 2018), such as passive microwave snow cover products (Hao et al., 2018; Huang et al., 2016), different temporal and spatial information of snow cover (Dong and Menzel, 2016; Gafurov and Bárdossy, 2009); however, most of these studies focused on binary snow cover.

When clouds appear in consecutive days, the use of the before-mentioned data fusion technology would cause significant uncertainties in detecting snow cover from optical imagery. The primary advantage of passive microwave sensors is that they are capable of measuring microwave radiation emitted from the ground under the clouds and in darkness. Besides, passive microwave sensors, compared with active, have a large swath width and massive amount of daily observation data that extend for several decades (Cohen et al., 2015). Nowadays, passive microwave brightness temperature data have been widely applied in monitoring soil moisture (Qu et al., 2019), sea/lake ice (Peng et al., 2013), frozen soil (Han et al., 2015), and snow cover. Previous studies about snow cover usually focused on snow depth (Xiao et al., 2018; Che et al., 2008), snow water equivalent (Takala et al., 2011; Lemmetyinen et al., 2018) and snow cover area (Liu et al., 2018; Xu et al., 2016). All these studies on snow cover area were limited to binary information. Specifically, they involved the application of seven common passive microwave snow cover mapping algorithms, Grody's algorithm (Grody and Basist, 1996), Kelly's algorithm (Kelly, 2009), Singh's algorithm (Singh and Gan, 2000), Hall's algorithm (Hall et al., 2002), Neal's algorithm (Neale et al., 1990), the FY3 algorithm (Li et al., 2007), and the South China algorithm (Pan et al., 2012), all of which utilize different thresholds for the brightness temperature to identify binary snow cover. Recently, Xu et al. (2016) applied the brightness temperatures of different channels and their linear combinations into the Presence and Background Learning (PBL) algorithm for identifying global binary snow cover.

Because of the effect of environmental factors (such as vegetation, topography, and wind) on snow cover distribution results in a vast heterogeneity, snow cover monitoring still bears larger uncertainties when only using passive microwave data. These large uncertainties may result from "patch" (shallow/discontinuous) snow cover and coarse resolution (25 km) (Xiao et al., 2018). Albeit with its coarse resolution, the capability of detecting snow cover in the presence of clouds makes passive microwave sensors an effective snow cover monitoring tool. Daily time-series and full space-covered sub-pixel snow cover area data are urgently needed for climate and reanalysis studies. Thus, it is necessary to derive high resolution fractional snow

https://doi.org/10.5194/tc-2019-280
Preprint. Discussion started: 7 January 2020

cover that can describe snow cover distribution patterns and capture its rapid evolution processes. Brodzik et al. (2018b) recently published the Calibrated Enhanced-Resolution Passive Microwave Daily EASE-Grid 2.0 Brightness Temperature data (see section 2.1 below), which have high spatial resolution (3.125 km, 6.25 km) depending on frequency (Brodzik et al., 2018a; Long and Brodzik, 2016). This resolution enhanced passive microwave data provides an opportunity for fractional snow cover estimation.

The main objective of this study is to develop a feasible method utilizing the enhanced-resolution passive microwave brightness temperature to predict daily fractional snow cover with a 6.25 km resolution. The datasets used in this study include the enhanced-resolution passive microwave data, ground-based measurements, MODIS snow cover and land cover products, topographic data are described in section 2. Section 3 details the proposed retrieval algorithm with the random forest as a retrieval function. Section 4 presents the results from the methods comparison, evaluation, and validation experiments. Finally, section 5 discusses the possible factors that affect the accuracy of the fractional snow cover estimates derived from passive microwave data.

2. Datasets

2.1 The enhanced-resolution passive microwave data

The NASA Making Earth System Data Records for Use in Research Environments (MEaSUREs) program provides one new version of passive microwave brightness temperature data called the Calibrated Enhanced-Resolution Passive Microwave Daily EASE-Grid 2.0 (Equal-Area Scalable Earth Grid) Brightness Temperature. These passive microwave gridded data use the Level-2 satellite records from multiple passive microwave sensors, time span from 1978 to mid-2017 (Brodzik et al., 2018b). This enhanced-resolution data can be downloaded from National Snow and Ice Data Center (NSIDC, https://nsidc.org/data/NSIDC-0630/versions/1). We used data from 2010 to 2017 (January–February only) to explore the feasibility of estimating fractional snow cover using passive microwave data. The Special Sensor Microwave/Imager (SSMIS) sensor (F-16) used in the present study offer three channels (19-, 37- and, 91-GHz) in both horizontal (H) and vertical (V) polarization and 22-GHz with vertical polarization. These datasets were gridded into EASE-Grid 2.0 projections at two spatial resolutions (19-, 22-GHz with 6.25 km; 37-, 91-GHz with 3.125 km). In order to avoid as much as possible wet snow effects, only observations from descending orbit (morning, 03:52) were used (Derksen et al., 2000). To unite resolution, a bilinear interpolation was used to aggregate the 3.125 km spatial resolution data to 6.25 km.

2.2 Ground measurements

Although ground measurements of snow cover have limited spatial representativeness in passive microwave coarse spatial resolution, the in-situ measurements are still the most authentic and reliable data for snow depth estimation or snow cover

https://doi.org/10.5194/tc-2019-280
Preprint. Discussion started: 7 January 2020

detection (Chen et al., 2018; Sturm et al., 2010). The ground measurements from the Global Historical Climatology Network-Daily (GHCN-Daily) data were used to assess the snow cover detection capability. The GHCN-Daily dataset is provided by National Climatic Data Center (available in http://doi.org/10.7289/V5D21VHZ); it integrates daily observations from approximately 30 different data sources. The new version data, updated on June 13, 2018, contains measurements from over one hundred thousand stations worldwide. These stations record a variety elements of meteorological observation, including snow depth and snowfall (Menne et al., 2012a; Menne et al., 2012b). Data for more than 50000 measurement sites across Canada and America were collected, all available records from these sites were included in this study.

2.3 MODIS land surface products

2.3.1 Snow cover product

Because of its wide application, high accuracy (Hall and Riggs, 2007; Zhang et al., 2019; Coll and Li, 2018), and high spatiotemporal resolution (1-day; 500-m), MODIS snow cover products were considered as the most suitable reference data. The accuracy of the MODIS snow cover products (version 6) has been improved compared to version 5 (Dong et al., 2014; Huang et al., 2018). The most noticeable change for version 6 is that the Normalized Difference Snow Index (NDSI) snow cover has replaced fractional snow cover, while the binary snow covered area (SCA) data is no longer available (Riggs and Hall, 2016). A snow cover detection method using NDSI was applied in version 6 to alleviate commission errors (Riggs et al., 2017). The NDSI index contributes to distinguish snow from other surface features and to describe the presence of snow (Hall et al., 1998; Hall et al., 2001). These products are available from NSIDC website (MOD10A1: https://nsidc.org/data/MOD10A1; MYD10A1: https://nsidc.org/data/MYD10A1). The local equatorial crossing times of MODIS onboard the Terra and Aqua satellites are approximately 10:30 a.m. and 01:30 p.m., respectively. In the present study, both MOD10A1 and MYD10A1 NDSI snow cover products were used to generate reference fractional snow cover over North America. NDSI snow cover data were firstly converted to binary snow cover in order to aggregate into the fractional snow cover data with a 6.25 km spatial resolution (see section 3.2).

2.3.2 Land cover product

Generally, the retrieval accuracy of snow cover parameters strongly depends on the land cover types (Xiao et al., 2018; Kuter et al., 2018; Dobreva and Klein, 2011; Huang et al., 2018). Thus, we indirectly considered the land cover effect when estimating fractional snow cover by establishing retrieval models on different land cover classes derived from MODIS land cover data (2010 - 2017). MODIS Land Cover Type Yearly Product (MCD12Q1, version 6) incorporates five different classification schemes and is globally available at a 500-m spatial resolution from 2001 to the present (https://search.earthdata.nasa.gov/). The International Geosphere–Biosphere Program (IGBP) classification scheme categorizes land cover into 17 classes (Sulla-Menashe and Friedl, 2018). In the study, MCD12Q1 data was resampled into the

https://doi.org/10.5194/tc-2019-280
Preprint. Discussion started: 7 January 2020

6.25 km grid using a simple majority method, and then it was integrated into five classes: forest, shrub, prairie, bare land, and water (refer to Xiao et al. (2018)). The fractional snow cover retrieval models were established for the previously mentioned four land cover types, except for water.

2.4 Topographic data

Previous studies have demonstrated that topography plays an important role in snowpack distribution (Dai et al., 2017) and snow evolution (Savoie et al., 2009). The ETOPO1 data was used as topographic auxiliary data. ETOPO1 has a 1 arc-minute spatial resolution and was developed by National Geophysical Data Center, National Oceanic and Atmospheric Administration (Amante and Eakins, 2009). This data is available from the website (https://data.nodc.noaa.gov/cgi-bin/iso?id=gov.noaa.ngdc.mgg.dem:316). This study considered not only elevation but also slope and aspect factors. The elevation was directly acquired from ETOPO1, which was re-projected and resampled into the grid at 6.25 km spatial resolution. The slope and aspect data were processed by ArcGIS 10.5 as a derivative product of ETOPO1 data. Fig. 1 shows the elevation pattern of our study region, North America.

3. Methodology

Microwave radiation constantly emitted from the substratum can be measured by passive microwave sensors. However, the overlying snow pack attenuates the upward microwave radiation (Chang et al., 1987). This microwave radiation attenuation was mainly dominated by volume scatter relying on the properties of the snow cover. However, previous studies have demonstrated that the snow properties and the distribution of snow cover show great heterogeneous and may be influenced by many factors (Xiao et al., 2019), including, but not limited to, the most prevalent land-cover (Che et al., 2016; Kim et al., 2019), topography (e.g., elevation, topographic relief) (Smith and Bookhagen, 2016; Revuelto et al., 2014), time (Sturm et al., 2010; Dai et al., 2012) and climatic conditions (e.g. wind speed, near-surface soil temperature and air temperature) (Dong et al., 2014; Grippa et al., 2004; Josberger and Mognard, 2002). As a result, the more covered area or the more mass magnitude of the snowpack, the less upwelling microwave radiation was received by the satellite sensors (Chang et al., 1987; Dietz et al., 2011; Saberi, 2019).

3.1 Overview

In order to develop a fractional snow cover prototype retrieval method combined with optical and passive microwave data, we only used the January and February datasets, because during this period the snow cover areas reach its maximum and the snowpack properties are relatively stable (Xiao et al., 2018). The influential factors as mentioned above, including topography factor, land cover, location and time, were indirectly or directly considered during the retrieval of the fractional snow cover. So far, many researchers have applied machine learning techniques in snow cover parameters retrieval to explore

https://doi.org/10.5194/tc-2019-280
Preprint. Discussion started: 7 January 2020

the relationship between passive microwave signal and snow property (Xiao et al., 2018; Tedesco et al., 2004). Here, random forest regression (described in section 3.4.4) was selected as the retrieval function to mine the relationship between passive microwave brightness temperature and fractional snow cover. Fig. 2 shows an overview of the workflow that consists of four parts:

First, a ground "truth" observation is necessary for producing snow cover area in sub-pixel. Under clear-sky conditions, the reference fraction of snow cover were generated within a 6.25-km pixel cell by applying the aggregation method to the MODSI binary snow map (see section 3.2). The reference fractional snow cover data was divided into three parts: the data from 2011 to 2016, used in the training stage; the data from 2010, used in the testing stage; and the 2017 data, used in evaluation stage.

Second, to the best of our knowledge, there are no researchers have developed fractional snow cover retrieval methods using passive microwave data. Thus, a sensitivity experiment of input variables is needed. The input parameters were selected based on the tests described in section 3.3.1.

Third, many studies have found that the separate estimation of fractional snow cover (Dobreva and Klein, 2011) and snow depth (Xiao et al., 2018) on different land cover types has better results than those obtained from combined retrieval model. Hence, the random forest models were separately developed for four land cover types.

Fourth, the last stage is the evaluation and validation of the established model. The data from 2010 were used to assess the performance of four different approaches for estimating fractional snow cover. Additionally, the independent datasets in 2017 were employed to evaluate the performance of the random-forest-based retrieval algorithm for four land cover types. The independent validations of snow cover detection capability were conducted using the 2017 retrieval results and station snow depth measurements across North America and compared with the results of Grody's snow cover mapping algorithm.

3.2 Preprocessing of MODIS snow cover products

The reference fractional snow cover data obtained from the interpretation of MODIS snow cover products is the base data for our work. The top priority issue is to produce daily binary snow cover area from NDSI snow cover. Previous snow cover detection studies recommend a 0.4 NDSI threshold on global and regional scale snow cover investigation (Parajka et al., 2012; Hall et al., 1995); However, for the new version of MODIS snow cover products, several previous researches employed a threshold of NDSI > 0 to identify snow cover (Dong et al., 2014; Riggs et al., 2017; Huang et al., 2018). The NDSI of other features (e.g., cloud-contaminated pixels at the edges of cloud, salt pans, and the pixel with very low visible reflectance) can also be greater than 0 (Riggs et al., 2017). For this reason, Zhang et al. (2019) demonstrated that a 0.1 NDSI threshold is more reasonable than 0.4 for snow cover identification in no-forest regions, whereas, forest-covered regions lack enough station measurements to do a reliable and complete evaluation. MODIS snow cover performs better in no-forest than forest-covered landscapes, in which it is with less accurate for snow cover identification (Hall and Riggs, 2007; Parajka et

https://doi.org/10.5194/tc-2019-280
Preprint. Discussion started: 7 January 2020

al., 2012).

In this study, the NDSI thresholds of 0.1, in no-forest-covered area, and 0.4, conservatively chosen for forest-covered areas (Riggs and Hall, 2016), were used for determining "snow-covered" or "snow-free". The original NDSI snow cover layer classes were reclassified into five types: snow-covered, snow-free, water, cloud, and fill (refer to Table S1 in Appendix). In addition, MCD12Q1 data (500-m) were used as auxiliary data to mask water bodies (Fig. 3) to alleviate the uncertainty caused by frozen water bodies when using passive microwave data to detect snow cover (Tedesco and Jeyaratnam, 2016). The MODIS binary snow cover data were generated based on NDSI snow cover basic quality assessment (QA), with values of 0 (best), 1 (good) and 2 (OK) (Liang et al., 2017).

Even if MODIS snow cover products have a high spatiotemporal resolution and overall accuracy of snow cover detection (85% ~ 99%) (Parajka et al., 2012; Tran et al., 2019; Zhang et al., 2019), the cloud effect hinders its widespread applicability. Previous studies reported that clouds could cover more than 40% of the MODIS snow cover data, in some cases even exceeding 60% (Dong and Menzel, 2016; Yu et al., 2016; Parajka and Blöschl, 2006). Cloud removal processing is essential to mitigate cloud obstruction of MODIS products. The cloud removal method combining the MOD10A1 and MYD10A1 snow cover products, proposed by Gafurov and Bárdossy (2009), was adopted. This method consists of two main filters as shown in Fig. 3:

1) Combining snow cover images from two sensors on a given day. The first simple filter was applied under the assumption that snowmelt and snowfall did not occur within the two sensor observations. Whether a pixel on Terra or Aqua is observed as snow cover or snow-free, the pixel in the combined image (MCD10A1) will be assigned the same ground status (Eq. 1). The results showed about 3% of cloud cover was removed compared to MOD10A1 (Gafurov and Bárdossy, 2009).

2) Short-term temporal filter. If the status of a pixel in MCD10A1 is cloud and the preceding and succeeding days are both snow-covered (or snow-free), the cloud pixel in the current MCTD10A1 image will be assigned a snow-covered status (or snow-free) (Eq. 2). Compared to the first filter, this short-term temporal filter may strikingly reduce the number of days (10 ~ 40%) for cloud coverage and increase in overall accuracy for snow cover detection (Gafurov and Bárdossy, 2009; Tran et al., 2019).

$$S_{(output,t)} = max\left(S_t^{Aqua}, S_t^{Terra}\right) \quad (1)$$

$$S_{(output,t)} = 1 \ \ if\left(S_{(t-1)} = 1 \ \ and \ \ S_{(t+1)} = 1\right) \quad (2)$$

where, t is the time and S represents the ground status observed in the image (0 or 1). 0 notes cloud presence; 1 indicates snow-covered or snow-free.

Theoretically, the MODIS fractional snow cover map should calculate the percentage of snow cover in a strictly delimited area of the passive microwave pixel. Calculation areas should be in a larger feet than the pixel resolution to avoid

https://doi.org/10.5194/tc-2019-280
Preprint. Discussion started: 7 January 2020

MODIS geolocation uncertainties (Wolfe et al., 2002; Dobreva and Klein, 2011). In this study, a window of 15*15 pixels of MODIS binary snow cover data (MCTD10A1; 500-m) was used for calculating the fraction of snow cover in a 6.25-km pixel. We decided to adopt the most rigorous pixel filter, in which one clouded pixel can not be allowed within a 15*15 pixels window. It is somewhat different from previous study that allowed 10% of clouds (Dai et al., 2017).

3.3 Sensitivity study

3.3.1 Selecting input variables

After determining the retrieval function, a major challenge is to select the fewest number of variables and then provide an efficient estimation model (Mutanga et al., 2012). Many factors influence snowpack distribution and it is unrealistic to consider all factors into the snow cover properties estimation. Therefore, we conducted six scenarios to evaluate and finally screen the input variable. According to previous study, topographic factors (DEM, slope, aspect) (Revuelto et al., 2014) and location information (longitude and latitude) (Xiao et al., 2018; Sturm et al., 2010) were directly take as the basic input variables. Additionally, the passive microwave brightness temperature (19-GHz, 37-GHz, and 91-GHz; both H and V polarization) (Xiao et al., 2018; Xu et al., 2016) and the difference of brightness temperature between different channels (Xu et al., 2016; Liu et al., 2018) were also considered (listed in Table 1). The 22-GHz channel was excluded because it is sensitive to water vapor.

The decision tree was established using all variables shown in Scenario-1 (Table 1), which was used to compare with the following five scenarios in terms of prediction performance and efficiency. Note that these 19 input variables were determined using the Correlation Attribute Evaluation method in WEKA 3.8.3 (Waikato Environment for Knowledge Analysis) data mining software. This method evaluates the worth of the attribute by measuring the correlation between the attribute and the target (Frank et al., 2004; Eibe Frank, 2016). The brightness temperature and its linear combination can also be directly used to detect snow cover (Xu et al., 2016); Thereby, Scenario-2 only contains brightness temperature and its linear combination without considering location and topographic factors effects. Wiesmann and Mätzler (1999) reported that vertical and horizontal polarization are dominated by scattering and snow stratigraphy, respectively. Thus, Kim et al. (2019) only assimilated vertical polarization with an ensemble snowpack model to estimate snow depth. In Scenario-3, we evaluated the performance of the retrieval model established by only using the brightness temperature in 19-GHz, 37-GHz and 91-GHz (V polarization). In the Scenario-4, we used similar input variables to those used for snow depth estimation in Xiao et al. (2018), and examined whether these same parameters can or not estimate fractional snow cover. Correspondingly, in Scenario-5, we used the basic input variables coupled with brightness temperature linear combination for fractional snow cover retrieval.

The importance rank of the input variable was generated during the training stage of the random forest model (refer to section 3.4.4). Based on the importance rank, Mutanga et al. (2012) implemented a backward feature elimination method to progressively eliminate less important variables; Nguyen et al. (2018) summarized the grade of variable and selected the top

https://doi.org/10.5194/tc-2019-280
Preprint. Discussion started: 7 January 2020

eight important variables as the input variables in training model. Similarly, we assessed the importance of input variables on four land cover types using the same size of training sample (15000) (Xiao et al., 2018). We then counted the times each variable is in the ranked top nine important variables (summarized in Table S2 in the Appendix). Scenario-6 shows the selected the top nine important variables (listed in Table 1). By analyzing the performance of models established using the variables in six scenarios, we will select an optimal combination of input variable for the fractional snow cover retrieval model (see section 4.1.1). All input variables were normalized to [0, 1].

3.3.2 Determining sample size

Although the random forest method can avoid overfitting (Breiman, 2001), it is important to evaluate the sensitivity to sample selection types and the size of the training sample (Belgiu and Drăguţ, 2016; Millard and Richardson, 2015; Nguyen et al., 2018; Colditz, 2015). The performance of predicted models trained by machine learning methods is strongly dependent on the quality of the training sample (Dobreva and Klein, 2011). A good quality training sample indicate that the sample data cannot be biased towards a certain value. The distribution of the fractional snow cover value from our dataset shows that more than 70% of the value are near 0 and 1. Hence, the use of random selection or equal proportional selection method (Millard and Richardson, 2015; Lyons et al., 2018; Nguyen et al., 2018) would hinder the interpretation of the final fractional snow cover estimation model by making the estimation less accurate. Therefore, we adopted the stratified random sampling as sample selection strategy (Xiao et al., 2018; Dobreva and Klein, 2011). Stratification was performed on the value of fractional snow cover with an increment of 0.01.

From previous studies, we know the sample size, approximately 0.25% of the total study area, was adopted by Colditz (2015) when using the random forest method. Moreover, this value has been evaluated in optical and active remote sensing studies (Nguyen et al., 2018; Du et al., 2015). In this study, we separately generated the training sample datasets from 0.15% to 0.35% of the total cover area of each land cover class (in 0.05% increments). Then the sensitivity tests were carried out for four land cover types; in this way, the training dataset would represent the values of fractional snow cover categories for each land cover type (see section 4.1.2). All the selection operations were completely random.

3.4 Description of different estimation methods

In this study, we compared the random forest method with the other three methods for retrieving fractional snow cover, including linear regression, ANN, and MARS. It should be noted that the input variables of the four methods are the same and are selected by the sensitivity test (see section 3.3.1 and 4.1.1).

3.4.1 Linear regression

A sub-pixel snow cover area estimation method has been developed for optical remote sensing studies by establishing a

https://doi.org/10.5194/tc-2019-280
Preprint. Discussion started: 7 January 2020

linear relationship between NDSI and fractional snow cover derived from high resolution snow cover map (Salomonson and Appel, 2004; Salomonson and Appel, 2006). This regression method has been applied in generating the current standard MODIS fractional snow cover product Collection 5. This multiple linear regression method, which uses least squares, was employed as a reference method to estimate fractional snow cover from passive microwave data. This method was complete in WEKA 3.8.3 and do not use any attribute selection method. In Appendix, we presented the linear regression formulas of fractional snow cover estimation for the four land cover types (Eq. S-1 and Table S6).

3.4.2 ANN

ANN is a popular machine learning technique that has been widely applied in remote sensing studies. Tedesco et al (2004) developed a snow water equivalent and snow depth retrieval algorithm based on an ANN technique using passive microwave brightness temperature. ANN also was involved in Xiao et al. (2018) study to derive snow depth, and Kuter et al. (2018) and Czyzowska-Wisniewski et al. (2015) study to retrieve fractional snow cover from MODIS data.

ANN consists of an input layer, one or more hidden layers, and an output layer (Hecht-Nielsen, 1992). The network with multiple perceptron can easily handle the nonlinear relationship between the input and output without any prior knowledge (Haykin, 2009). The inputs of each neuron are multiplied and summed by the connection weight, and then the output results are computed through a nonlinear logistic sigmoid transfer function. For numerical data, the transfer function in WEKA substitutes the pure linear unit function for the logistic sigmoid.

Apart from the data preprocessing, a crucial step in this process is to design and optimize the ANN network structure for a better estimation performance and good generalization capability (Kuter et al., 2018). Kuter et al. (2018) demonstrated that multidimensional function modeling can be done successfully with one hidden layer network. All parameters were set as default except for the learning rate, which was optimized through a simple trial-and-error method. From the accuracy index and the modeling speed aspect, Table S3 in the Appendix show that 0.2 as the learning rate generated the best performance of the ANN-retrieval model.

3.4.3 MARS

MARS technique has been applied in quite plenty of studies and in many fields, e.g., classification and mapping (Quirós et al., 2009), atmosphere correction (Kuter et al., 2015), pile drivability prediction (Zhang and Goh, 2016), and fractional snow cover estimation (Kuter et al., 2018). Unlike ANN, the modeling process of MARS is flexible and straightforward. Friedman (1991) first proposed the MARS technique that organizes a simple model for the complex and high-dimensional relationship between the input variables and the target by having simply piecewise linear polynomials (known as basis functions (BFs)) smoothly connected. The ranges of the input variables are cut into a series of sub-ranges by the knots that is connection points for two pieces of BFs. A simple BFs format of MARS is expressed as showing in Eq. 3. $max(\cdot)$ indicates that only positive

https://doi.org/10.5194/tc-2019-280
Preprint. Discussion started: 7 January 2020

parts are take; otherwise, it is assigned as zero. τ is a univariate knot.

$$max(0, x-\tau) = \begin{cases} x-\tau, & if \ \ x > \tau \\ 0, & otherwise \end{cases} \quad (3)$$

The MARS method involves two stages (forward phase and backward phase) for establishing a regression model. In the forward phase, the BFs were generated by the stepwise search of all univariate candidate knots and all variables interactions. These adopted knots and its corresponding pair of BFs should produce the greatest decrease in residual error. The BFs were successively added to the model until the maximum number of BFs was reached. As a result, the model is over-fitted and complicated. In the backward phase, the redundant BFs that make the least contributions for model predictive is completely excluded from the regression model. These two phases are an iterative process (Kuter et al., 2018; Zhang and Goh, 2016).

Two important parameters of MARS determine the model "growing" and "pruning" processes. The first is the maximum number of basis functions (max_BFs), and the second is the maximum degree of interactions among the input variables (max_INT) (Kuter et al., 2018). Kuter et al. (2018) reported that the increase in the structural complexity of the model does not significantly contribute to improve the performance of the MARS model. We did several tests to optimize the structure of MARS and found that more complex structure had a longer modeling time, but the performance of the model did not significantly improve. Specifically, the modeling time of the complex structure (max_BFs = 100, max_INT = 2) is more than four times than that of the simple structure (max_BFs = 40, max_INT = 2). Thereby, following Kuter et al. (2018), the simple structure was chosen. We implemented an open MARS MATLAB source code available from Jēkabsons (2016) for fractional snow cover estimation. These codes were compiled on a 2.40 GHz Intel Xeon CPU server.

3.4.4 Random forest

Random forest is an ensemble learning method, which has drawn many researchers' attention because it is more efficient and robust than the single method (Breiman, 2001). As a classifier, random forest has been successfully used to detect snow cover (Tsai et al., 2019), land cover (Rodriguez-Galiano et al., 2012), and woody invasive species (Kattenborn et al., 2019). The random forest regression method also provides a successful estimation of land surface temperature (Zhao et al., 2019), biomass (Mutanga et al., 2012), and soil moisture (Qu et al., 2019).

Random forest built a large series of decision trees by applying the bootstrap sampling method. In the training stage, each tree grows by randomly selecting several variables and samples from input datasets (Mutanga et al., 2012). The input data was repeatedly split into training and test data using the bootstrapping method. Each randomly selected bootstrap sample in each iteration contains approximately 2/3 of the input elements. The remaining data, called out-of-bag (OOB) data, is used for validation. The predicted value of OOB data is produced from all produced trees results and the OOB error is calculated. For classification, the output is determined by voting the results from all decision trees; whereas for regression, the output results is by averaging. The random forest was performed in WEKA 3.8.3. Several attempts to optimize the parameters of random

https://doi.org/10.5194/tc-2019-280
Preprint. Discussion started: 7 January 2020

forest structure failed. Thus, all the parameters used were the default values here.

3.5 Snow cover identification

The microwave radiation characteristics of precipitation, cold deserts and, frozen ground are similar to that of snow cover (Grody and Basist, 1996). As a result, the snow cover area is likely to be overestimated. Grody and Basist (1996) proposed a snow cover identification algorithm, which can distinguish snow cover from precipitation, cold desert, and frozen ground. Consequently, many researches used Grody's algorithm and its derivative algorithm to detect snow cover (Che et al., 2008; Xiao et al., 2018; Wang et al., 2019). Liu et al. (2018) reported that the assessment results of different passive microwave snow cover detection algorithms and showed Grody's algorithm had a higher precision (positive predictive value) than other algorithms. Due to the highest frequency in this study is 91-GHz instead of 81-GHz in SSMIS sensors, we adopted the revised snow cover decision tree of Grody's algorithm (Table 2) (Che et al., 2008).

There are two main objectives for using the revised Grody's algorithm (hereafter referred to Grody's algorithm) in this work. The first is to compare the snow cover identification capability of the proposed fractional snow cover estimation algorithm with respect to ground snow depth measurements (see section 4.4); On account of this algorithm's special capability to distinguish the non-snow scatterer (i.e., precipitation, cold desert, and frozen ground), the second purpose is to assess the affect of non-snow scatterer in estimating fractional snow cover. In both optical and microwave remote sensing research, the capability assessment of snow-free detection has been regularly neglected in most of the previous snow cover detection studies.

3.6 Validation of snow cover identification

When using the in-situ snow depth (or snow water equivalent) measurements to quantitatively validate the accuracy of snow cover area data, the first challenge is how to convert snow depth into binary snow cover using an appropriate threshold. Numerous values of depth threshold have been suggested in published studies: 0 cm (Parajka et al., 2012); 1 cm (Zhang et al., 2019), 2 cm (Brown and Derksen, 2013; Gascoin et al., 2019), 2.5 cm (Hori et al., 2017), 3 cm (Hao et al., 2018; Xu et al., 2016), 4 cm (Huang et al., 2018; Wang et al., 2008), 5 cm (Liu et al., 2018), and even 15 cm (Gascoin et al., 2015). Because of this vigorous disagreement in the depth threshold value, Gascoin et al. (2019) conducted a sensitivity experiment that tested the agreement between in-situ measurement and optical snow cover area products. Similarly, the sensitivity of passive microwave snow cover identification results to the snow depth was also tested by computing the accuracy metrics with snow depth value increasing from 0 cm to 10 cm.

The next problem is to determine the threshold for converting fractional snow cover to binary snow cover. Up to now, there are few studies on fractional snow cover from passive microwave pixel-level. Dai et al. (2017) took the grid consider as snow cover if the fractional snow cover (25-km) is larger than 10%. Additionally, if the fraction of snow cover is less than 0.25, the snow water equivalent (SEW) is set to 0 mm for correcting snow cover area in the daily SWE product according to

https://doi.org/10.5194/tc-2019-280
Preprint. Discussion started: 7 January 2020

Luojus et al. (2018) study. However, 0.5 often is the used threshold of fractional snow cover adopted in optic remote sensing studies (Hall and Riggs, 2007). Sensitivity experiments of fractional snow cover similar to ground-based snow depth were employed in order to obtain the optimum conversion threshold. Both sensitivity experiments were carried out using 2017 bare land type datasets in section 4.4.

3.7 Performance accuracy assessment

When evaluating the estimation performance of fractional snow cover in section 4.1-4.3, we used conventional accuracy metrics: correlation coefficient (R; Eq. 4), mean absolute error (MAE; Eq. 5) and root mean squire error (RMSE; Eq. 6). $\overline{x}$ is the mean value of all predicted values x_i; $\overline{y}$ is the mean value of all target values y_i; n denotes the number of used data.

$$R = \frac{\sum_{i=1}^{n}(x_i - \overline{x})\,(y_i - \overline{y})}{\sqrt{\sum_{i=1}^{n}(x_i - \overline{x})^2 \sum_{i=1}^{n}(y_i - \overline{y})^2}} \quad (4)$$

$$MAE = \frac{1}{n}\sum_{i=1}^{n}|x_i - y_i| \quad (5)$$

$$RMSE = \sqrt{\frac{1}{n}\sum_{i=1}^{n}(x_i - y_i)^2} \quad (6)$$

We not only evaluated the predicted accuracy of fractional snow cover, but also assessed the snow cover identification performance (see section 4.4). Six accuracy assessment indexes were used for snow cover detection capability analysis: overall accuracy (OA), precision (a.k.a. positive prediction value), recall, specificity (a.k.a. true negative rate), F1 score, and Cohen's kappa coefficient. OA refer to the proportion of correctly classified pixels as snow-covered and snow-free. The F1 score is a weighted average measurement of precision and recall ranging from 0 to 1 for measuring the accuracy of binary classification. Cohen's kappa coefficient measures the agreement between the snow cover products and ground measurements. All of these indexes can be calculated from the confusion matrix (Table 3). OE is the omission error; CE is the commission error.

4. Results analysis

4.1 Sensitivity in the training sample

4.1.1 Influence of input variables on model performance

To better understand which input variables have a relationship with fractional snow cover and the variable combination can improve the retrieval model performance, we evaluated the results from 24 random forest fractional snow cover retrieval models (4 types * 6 scenarios). The data used for variable sensitivity tests in this part merely involved two years (2014-2015) since 91-GHz horizontal polarization data is missing over the area south of 50° N in 2016-2017. The OOB error and 10-fold cross-validations error were used to measure the performance of fractional snow cover retrieval models in each scenario (Mutanga et al., 2012). Table 4 shows the results of six scenarios on bare land type datasets.

https://doi.org/10.5194/tc-2019-280
Preprint. Discussion started: 7 January 2020

The variable selection tests are used to seek a better combination of different variables (Table 4). At first glance, Scenario-3, which only involves vertical polarization data, yields the smallest R (0.590) and the largest MAE (0.197) and RMSE (0.248) of OOB error and also for 10-fold cross validation error (R: 0.596; MAE: 0.197; RMSE: 0.246). When compared to the other five scenarios, Scenario-3 had the worst performance, which may be due to no more available information from input variables that can be fully exploited (Xiao et al., 2018). Scenario-2, that only contains passive microwave brightness temperature data that is nearly same as the variable used in Xu et al.(2016) study, had the second worst performance. It has proven that the location information and topographic factors play a crucial role in snowpack distribution (Revuelto et al., 2014; Czyzowska-Wisniewski et al., 2015; Sturm et al., 2010). The major difference between Scenario-1, 4 5, 6 and Scenario-2, 3 (Table 1) is the consideration of the basic input variables (location information and topographic factors). Thereby, the comparison results (Scenario-1, 4 5, 6 vs. Scenario-2, 3) further indicate that the effect of location information and topography need to be considered for snow parameters estimation. Even though the input variables of Scenario-6 is selected by importance, this setting generated the worse performance, with the low R, the great MAE and RMSE. As for Scenario-1, 4 and 5, they gave better results; there were no obvious differences in R, MAE and RMSE values for the four land cover types tests (Table 4; Table S4 and S5 in Appendix). This comparison indirectly indicates that the variables used in Scenario-1 have information redundancy and slightly weaken the efficiency of the random forest retrieval model. While the selection method of Scenario-4 and Scenario-5 performed well (in modeling time and accuracy of predicted target), only one scenario was selected, the other one can be used as an alternative in the future. Finally, the variable combinations in Scenario-5 were selected for further analysis.

4.1.2 Determination of sample size

The datasets from 2014-2016 were used to examine the sensitivity to training sample size. The used accuracy metrics are the same as in section 4.1.1. On account of the values and variation trends of the accuracy metrics of OOB error and 10-fold cross validation error are almost same, thus, only OOB error were shown in Fig. 4 and Figure S-1, 2, 3 (in the appendix). We compared the performance of random forest-based models altering the training sample size for the four land cover types.

Fig. 4 illustrates the R slow increase and the MAE and RMSE slight decrease with the training sample size increase from 0.15% to 0.25% on the shrub type. Meanwhile, the modeling time has a significant increase. As the sample size goes from 0.25% to 0.35%, the model shows a consistently accurate performance of fractional snow cover estimation (higher R and less MAE and RMSE). This finding appears to be consistent with previous studies (Colditz, 2015; Nguyen et al., 2018). An applicable and eligible sample selection scheme, which can achieve an acceptable target prediction accuracy level and an adequate execution time, is essential for the implementation of a random forest model with superior predictive capability. One noticeable distinction between the three sample sizes (0.25% ~ 0.35%) is the modeling time. Interestingly, the 0.3% training sample size had the lowest modeling time of the three sample size (Fig. 4). Figure S-1, -2, -3, show that this finding was not

https://doi.org/10.5194/tc-2019-280
Preprint. Discussion started: 7 January 2020

be coincidental. The explanation for the difference in modeling time is beyond the scope of this study and requires further research. We used the sample dataset covering 0.30% of the study area of each class as a suitable size to randomly select training samples. Subsequently, we extracted the training samples for each land cover type from the 2011-2016 dataset to establish the retrieval models.

4.2 Comparison of the four retrieval methods

In this section, the independent testing datasets from 2010 were used to assess the predictive performance of random forest-based models and the other three models (based on linear regression, ANN and MARS). When comparing the modeling time of the four methods (Table 5), linear regression shows the shortest time, with less-than 1 s for the four land cover types, followed by ANN that is approximately 51 s (forest), 22 s (shrub), 156 s (prairie) and 35 s (bare land). Random forest modeling times, are very close to ANN modeling times for each land cover type. By contrast, the MARS is the most time consuming, takes the longest time (about 6.5 hours) for the prairie type and the shortest (19 minutes) for the shrub type. The absolute value of the modeling time would vary under different computer capabilities.

Table 5 and Fig. 5 exhibit the results of the four retrieval methods for the four land cover types. The retrieval models of shrub type almost have the lowest RMSE in contrast with the other three land cover types for four methods (Table 5; cf. Fig. 5 and Figure S-4, 5, 6 in the Appendix). For forest (Table 5; Fig. 5 and 6), the random forest model has the highest R (0.916), lowest MAE (0.202) and RMSE (0.245), and no out-of-range records. The distribution and variation of MAE and RMSE for the four methods are nearly the same under different land cover types except for the shrub type (Table 5; Fig. 5). Apart from ANN, the ranking of results accuracy (MAE and RMSE) of the three algorithms on shrub test data also is the same as that under other land cover types (Random forest > MARS > linear regression). For the R, random forest shows the greatest value, followed by ANN, then MARS, and finally for most of the land cover types the smaller value is from the linear regression. As showed in Fig. 6, random forest (Fig. 6D) produced a relatively small number of overestimated (around 0) and underestimated (around 1) values compared with the other three models (Fig. 6A - 6C). The MAE (0.315) and RMSE (0.401) of ANN are greater than those of MARS (MAE = 0.208, RMSE = 0.254). The number of out-of-range estimated values of ANN (36.62%; 161260) is also greater than that of MARS (2.65%; 11667), which may be due to the fractional snow cover were seriously underestimated by the ANN method. The maximum and minimum of ANN and MARS on the forest type are 0.949 (-0.52) and 2.132 (-0.122), respectively. For the other three land cover types, the numbers of out-of-range pixels of the four methods have almost the same order (Random forest < ANN < MARS < linear regression).

The random forest-based models have the best performance with the highest R, and lowest MAE and RMSE (Table 5). Previous studies usually neglected to assess the rationality of estimated value (Liang et al., 2017; Wang et al., 2017; Hao et al., 2019; Masson et al., 2018). From Table 5, we know the random forest models for the four land cover types produced reasonable fractional snow cover values that range between 0 and 1. In comparison, the estimated fractional snow cover from the other

https://doi.org/10.5194/tc-2019-280
Preprint. Discussion started: 7 January 2020

three methods (linear regression, ANN and MARS) beyond this range. From the number of out-of-range records, the linear regression method generated the largest number of out-of-range fractional snow cover, more than 0.85 million pixels (18.69%). Although the number of out-of-range records of ANN (12.31%) is less than that of MARS (16.39%), both numbers exceed 0.5 million. The results from Kuter et al. (2018), which estimated fractional snow cover using MARS and ANN technique, also yielded the out-of-range values. The performance of the linear regression method in estimating fractional snow cover from passive microwave data is the worst; it shows the lowest R and the largest number of out-of-range records. Thus, nonlinear methods thus are first encouraged to use. Xiao et al. (2018) demonstrated the nonlinear relationship between passive microwave brightness and snow depth. Besides, De Lannoy et al. (2012) provided an exponential function for converting from snow water equivalent to fractional snow cover. Thus, it is reasonable for the nonlinear-relationship between fractional snow cover and passive microwave brightness temperature.

4.3 Evaluation of fractional snow cover

To further investigate the predictive capability of the random forest models, we conducted the evaluation using independent data from 2017 and analyzed the training and evaluation results for the four land cover types (Table 6, Fig. 7). As shown in Fig. 7A and 7a, the fractional snow cover values around 1 are distinctly underestimated and few are above the 1:1 line. The model for forest type exhibits the worst performance with the lowest R (0.932) and the highest RMSE (0.199) on validation dataset (Table 6). The retrieval model on the shrub type obtained the best performance on the validation data (R: 0.971; MAE: 0.142; RMSE: 0.167). In addition to forest, prairie shows more underestimation (around 0) and overestimation (around 1) records (R = 0.946, MAE = 0.163, RMSE = 0.198) than the other two land cover types (shrub and bare land) (Table 6; Fig. 7b - 7d). For shrub and bare land types (Fig. 7B, 7b, 7D and 7d), "true" fractional snow cover values in training or validation datasets are more distributed at two polar (0.0~0.3; 0.9~1.0). Fig. 8 shows the spatial patterns of MODIS composite binary snow cover (A), the calculated MODIS fractional snow cover (B), and the estimated fractional snow cover from passive microwave brightness temperature data (C). Fig. 8D presents a comparison example of these two fractional snow cover data and MODIS composite binary snow cover products in the Central Canada area on February 27th, 2017. The spatial pattern of estimated fractional snow cover from the proposed method seems to accurately capture the distribution of snow cover from MODIS under clear-sky condition (Fig. 8).

Thus far, we have evaluated the performance of random forest-based models on independent datasets from 2010 and 2017 on each land cover type. Seeing the results from the random forest (Table 5; Fig. 6D; Figure S-4 - 6; Fig. 7), we find the minimum estimates are higher than 0 and approximately 0.01. One possible reason is that the results output principle of random forest that the regression output results are obtained by averaging the results from multiple trees (see section 3.4.4) (Breiman, 2001; Belgiu and Drăguţ, 2016). Although MODIS snow cover products have high accuracy in snow cover identification (Tran et al., 2019), the estimated results indicate that a large number of fractional snow cover values were overestimated around 0

https://doi.org/10.5194/tc-2019-280
Preprint. Discussion started: 7 January 2020

and underestimated around 1. Some fractional snow cover estimates, in the individual pixel level, shows a large discrete distribution near the 1:1 line (Fig. 7). These misestimates appear not just in the results of the random forest model but also in the other three methods result (Fig. 6; Fig S-4 – 6 in the appendix). Other non-snow scatterers (precipitation, cold desert, frozen ground) may largely control the overestimates in low snow coverage region because in this regions the non-snow scatters were easily be misclassified into snow cover. As we all know, permafrost widely distributed in North America (Zhang et al., 2008), and it would offer great contributions to the misclassification of snow cover. The more detailed analysis of the misclassification is discussed in section 4.4. Moreover, the difference in satellite overpass time may also result in completely different snow cover information measured by satellite sensors. This difference can be easily neglected when using multi-sensor observations for data fusion. We know the difference of equator crossing time between MODIS sensors and passive microwave is close to 6.5 hours and 9.5 hours (refer to section 2.1 and section 2.3.1). Time-lapse photography from camera network was utilized to monitor snow processes in the Upper Rhine Region (Dong and Menzel, 2017b, a). According to Dong and Menzel (2017a) measurements, snow depth may exhibit great dynamics within hours under a snowstorm, continuous snowfall conditions, resulting in fractional snow cover changes rapidly (De Lannoy et al., 2012; Romanov and Tarpley, 2007). Thereby, the inconsistent observations occurred between the passive microwave sensor and MODIS.

4.4 Validation using ground measurements

In winter with clouds and snow cover, even after the implementation of the cloud removal and filling process for MODIS snow cover data, MCTD10A1 data still presents a large number of clouds (Fig. 8A; yellow). After applying the rigorous pixel filters (see section 3.2), there is very little snow cover data for further model training and results analysis in one imagery (Fig. 8B). Under the absence of reference MODIS fractional snow cover, how can we evaluate and validate the estimated fractional snow cover? Further analysis from the snow cover detection capability aspect was performed. The ground snow depth measurements were utilized to investigate the accuracy of snow cover identification from two snow cover data: the snow cover detected by Grody's algorithm and the fractional snow cover derived from random forest. We collected all available meteorological station snow depth measurements of 2017 (January and February) over North America, obtaining more than 311000 pairs of records, which include the snow depth measurements, the estimated fractional snow cover (hereafter referred to Random forest FSC) and, snow cover area derived from Grody's algorithm (hereafter referred to Grody's algorithm SCA).

The sensitivity to ground-based snow depth in snow cover detection results were tested by computing the accuracy metrics. Fig. 9 presents that the accuracy metrics vary with increasing snow depth. We can see that the accuracy metrics change significantly when snow depth exceeds 2 cm, and they reach a relative optimum value when snow depth is equal to 2 cm. Che et al. (2008) stated that snow cover can be detected by passive microwave sensors when snow depth is greater than 2 cm. Consequently, we adopted 2 cm as the optimum depth threshold to transform ground snow depth measurements to snow-covered or snow-free information. Moreover, we also conducted a series of sensitivity experiments were conducted to search

https://doi.org/10.5194/tc-2019-280
Preprint. Discussion started: 7 January 2020

the optimum threshold for converting fractional snow cover to binary snow cover (Fig. 10). Fig. 10 shows that recall and precision have opposite variation trends. F1-score is up to the maximum value when FSC =0.3. In additional, the other two indicators (OA, kappa) also reach the maximum value when the FSC value ranges between 0.3 and 0.4. As expected, 0.3 was taken as the conversion threshold for fractional snow cover. Nevertheless, the conversion thresholds of snow depth and fractional snow cover need to be optimized with more data in the future.

We used a 2 cm snow depth threshold and a 0.3 fractional snow cover threshold to calculate the confusion matrix for Grody's algorithm SCA and Random forest FSC against ground snow depth measurements (Fig. 11 and Fig. S-8). Fig. 11 illustrates that the overall accuracy of snow cover identification is significantly improved by 18%, from 0.71 for Grody's algorithm SCA to 0.84 for Random forest FSC, indicating that Random forest FSC results have a promising agreement with ground snow cover measurements (kappa = 0.67). For Random forest FSC, the precision (0.83) is lower than the recall (0.87), which means that snow cover area is more likely to be overestimated (CE = 0.17) than to be underestimated (OE = 0.13) with respect to in-situ measurements; For Grody's algorithm SCA, on the contrary, the precision (0.87) is larger than the recall (0.52). By utilizing the proposed method, the OE of snow cover identification is reduced by 71% in comparison to the OE for Grody's algorithm SCA. The snow cover identification accuracy for the four land cover types were illustrated in Figure S-8 (in the Appendix) by radar charts. Additionally, Fig. 8 provide a simple example of snow cover identification results of Random forest FSC (Fig. 8C) compared with MODIS composite binary snow cover product (Fig. 8A) on February 27th, 2017. From Fig. 8, we can find that the cloud-free area (snow-cover and snow-free area) in MODIS almost be captured by our estimated results.

Subsequently, we explored the influence of non-snow scatterer in estimating fractional snow cover. The CE of Grody's algorithm (CE = 0.13) is lower than that of Random forest FSC (CE = 0.17). Fig. 11 shows the overall snow-free identification capability of Grody's algorithm SCA (specificity = 0.92) is significantly superior to the Random forest FSC (specificity = 0.81), which is also apparent for the four land cover types (Figure S-8). It is possibly due to the Grody's algorithm filtering out non-snow scatter signature (precipitation, cold desert, and frozen ground) (Grody and Basist, 1996). Thereby, we counted the number of records that a pixel was detected as snow-free by the station and the Grody's algorithm but snow-covered by the Random forest FSC. The records, which are misclassified as snow cover by Random forest FSC but should be non-snow scatter component, account for 70% of total number of misclassification records by Random forest FSC. This proportion of forest, shrub, prairie and, bare land type is 78%, 93%, 71% and 67%, respectively (Table 7). In conclusion, the non-snow scatterer is the major source of snow cover misclassification for random forest FSC results (Grody and Basist, 1996). Therefore, it is necessary to first distinguish the scattering signature of snow cover from other non-snow scattering signatures when using passive microwave data to identify snow cover. Similar preprocessing has been applied into snow depth estimation to minimize its uncertainties (Xiao et al., 2018; Wang et al., 2019; Tedesco and Jeyaratnam, 2016).

https://doi.org/10.5194/tc-2019-280
Preprint. Discussion started: 7 January 2020

5. Discussions

5.1 Sensitivity to training sample size and quality

The size and quality of training samples may contribute to a large error at individual pixel level (Dobreva and Klein, 2011; Kuter et al., 2018; Nguyen et al., 2018; Belgiu and Drăguţ, 2016). Previous researches have investigated the sensitivity to sample size and sample quality (Nguyen et al., 2018; Colditz, 2015; Lyons et al., 2018). While some studies indicate that larger size of training sample improves the estimated results accuracy, we found that a training sample dataset covering about 0.3% of the total study area is enough to achieve high accuracy in the estimation of fractional snow cover. When comparing to previous sensitivity test on sample size (Nguyen et al., 2018), the major difference is taking the modeling time as one index in this study.

The estimation results of the random forest model on training and evaluation (test) datasets (section 4.2 and 4.3) showed that, in general, the prediction performance of random forest model is closely related to the quality of training sample. In this study's datasets, more records are located near the extreme values of the fractional snow cover (0 and 1). Thus, it is reasonable to employ the stratified random sampling (Dobreva and Klein, 2011) but not the proportional distribution of the target values suggested by previous studies (Nguyen et al., 2018; Millard and Richardson, 2015). Even then, the overestimation and underestimation often occur near 0.0 and 1.0 in training datasets (Fig. 7 A-D) and in evaluation datasets (Fig. 7 a-d). For future studies, it will be necessary to increase the amount of sample data by extending the study period to the snow accumulation and ablation stages (Xiao et al., 2018), in which have much of shallow snow and "patch" snow cover. Another option is using multi-source sensors data to generate the reference snow cover data, e.g., Sentinel-1 SAR (Synthetic Aperture Radar) data. By doing this, the proportion of the fractional snow cover value in training sample can be distributed as even as possible (Colditz, 2015; Jin et al., 2014; Lyons et al., 2018).

5.2 Effects of vegetation

Snow cover detection can be partially or completely obscured (or intercepted) by dense vegetation canopies. It bring great uncertainties on snow cover accurate detection (Che et al., 2016; Hall et al., 2001; Parajka et al., 2012). Forest cover is an influential factor that cannot be ignored in optical and microwave remote sensing studies (Metsämäki et al., 2005; Cohen et al., 2015). It is evident that the fractional snow cover retrievals almost have the least accuracy under forest type with respect to under other types (Table 5; Fig. 6 and Fig. 7). There are two reasons that can explain this error initially: one is the accuracy of the reference "true" fractional snow cover data in forested area (Riggs and Hall, 2016), the other is the microwave radiation attenuation caused by forest (Che et al., 2016).

Previous studies reported that lower accuracy of MODIS snow cover product is found in forest covered area and complex terrain (Hall and Riggs, 2007; Tran et al., 2019; Coll and Li, 2018). There are few studies that validate the accuracy of MODIS

https://doi.org/10.5194/tc-2019-280
Preprint. Discussion started: 7 January 2020

snow cover products in forested area (Parajka et al., 2012; Zhang et al., 2019). As for the NDSI threshold in forested area (section 3.2), we conservatively took 0.4 as the threshold. According to previous studies, our operation (merely using NDSI as the criterion) in forest-covered area would result in more commission error in compare with using the Normalized Difference Vegetation Index (NDVI) as auxiliary information (Hall and Riggs, 2007). The retrieval results indicated the threshold of NDSI in forested area needs to be optimized using numerous data (Riggs et al., 2017; Xin et al., 2012). In addition to the forest influence on MODIS data, forest hampers the upwelling microwave radiation emitted from the ground. Snow cover in forest areas can be divided into under-forest and over-forest snow cover (Xin et al., 2012). Thereby, the interference effects of evergreen forests and deciduous forests on snow cover are apparently different (Gascoin et al., 2019; Romanov and Tarpley, 2007). Additionally, in forested area, the observation way of optical and passive microwave sensor has great differences. Optical sensors capability to observe over-forest snow cover mainly depends on the vegetation canopy density (Kuter et al., 2018), while microwave can obtain information of snow cover under vegetation canopy (under-forest snow cover) (Che et al., 2016; Cohen et al., 2015). Overall, this combination of these two effects could cause the low accuracy in estimating fractional snow cover.

6. Conclusions

Many previous studies have focused on the estimation of fractional snow cover utilizing optical remote sensing imagery, which suffers from cloud contamination in data acquisition. In contrast, the microwave sensors offer attractive advantages of working under all weather conditions and around the clock. Thus, we tried to developed a algorithm for estimating fractional snow cover from the enhanced-resolution passive microwave brightness temperature data (6.25 km). The proposed algorithm took into account a series of influential factors, including topography, land cover, and location. Using the reference fractional snow cover stem from MODIS snow cover products as “true” observation, we established the fractional snow cover retrieval models for four land cover types (forest, shrub, prairie and bare land) inputting 12 variables selected by sensitivity experiments. Compared with the other three methods (linear regression, ANN and MARS), the random forest-based algorithm had the best performance with high accuracy (highest R, and lowest MAE and RMSE) and no out-of-range retrievals. The accuracy of the proposed algorithm were further assessed using MODIS reference fractional snow cover data of 2017, and the results showed that random forests models have a good retrieval performance in estimating fractional snow cover, with RMSE ranging from 0.167 to 0.207. In-situ snow depth measurements were used to validate the accuracy of the estimated results comparing them with the snow cover detection results from Grody’s algorithm. Snow cover identification capability of random forest is superior (OA =0.84, kappa = 0.67) to that of Grody’s algorithm, indicating that the proposed approach detects snow cover with considerable accuracy. Although the random forest models achieved an acceptable accuracy, the fractional snow cover are more likely to be overestimated (CE = 0.17) than to be underestimated (OE = 0.14). As Grody’s algorithm yielded good

https://doi.org/10.5194/tc-2019-280
Preprint. Discussion started: 7 January 2020

prediction on snow-free class, the effect of non-snow scatterer was evaluated on fractional snow cover predictions; it was found that more than 70% CE was caused by misclassifying non-snow scatterer (precipitation, cold desert, frozen ground) as snow cover.

Numerous studies have investigated the relationship between common snowpack physical properties (e.g., snow depth and water equivalent) and passive microwave brightness temperature in different frequencies and polarizations (Chang et al., 1987; Dietz et al., 2011; Kim et al., 2019; Xiao et al., 2018). However, this study was the first attempt to directly estimate fractional snow cover using passive microwave data. The results demonstrated that it is possible to obtain an estimated fractional snow cover directly with high accuracy from high spatial resolution passive microwave data (6.25-km) under all weather conditions. Thus, it would be an interesting research direction as an extension of the present fractional snow cover study. To reduce some of the limitations (e.g., forest effects) (Cohen et al., 2015) and deficiencies (overestimation and underestimation) faced in this study, the future works should pay more attention to the prediction of the fractional snow cover using passive microwave data. To the best of our knowledge, this study is the first attempt to establish a relationship between the microwave brightness temperature and the reference "true" fractional snow cover using machine learning methods. However, it presents strong limitations in the understanding of physical mechanism (Cohen et al., 2015; Che et al., 2016). Thereby, future work will try to use physical snowpack models and radiation transfer theory to explore the physical mechanism relationship between microwave brightness temperature and fractional snow cover (Pan et al., 2014).

Competing interests: We declare that we have no competing interests.

Acknowledgements: This work was supported by the National Natural Science Foundation of China Grant (41771379) and the National Key Research and Development Program of China Grant (2016YFA0600102).

Appendix

Supplementary material for this article is available in supplement.

References

Barnett, T. P., et al. : Potential impacts of a warming climate on water availability in snow-dominated regions, Nature, 438, 303-309, 10.1038/nature04141, 2005.

Belgiu, M., and Drăguţ, L.: Random forest in remote sensing: A review of applications and future directions, ISPRS Journal of Photogrammetry and Remote Sensing, 114, 24-31, 10.1016/j.isprsjprs.2016.01.011, 2016.

Berman, E. E., et al. : Daily estimates of Landsat fractional snow cover driven by MODIS and dynamic time-warping, Remote Sensing of Environment, 216, 635-646, 10.1016/j.rse.2018.07.029, 2018.

Bormann, K. J., et al. : Estimating snow-cover trends from space, Nature Climate Change, 8, 924-928, 10.1038/s41558-018-

https://doi.org/10.5194/tc-2019-280
Preprint. Discussion started: 7 January 2020

0318-3, 2018.

Breiman, L.: Random Forests, Machine Learning, 45, 5-32, 10.1023/a:1010933404324, 2001.

Brodzik, M., et al. : Best Practices in Crafting the Calibrated, Enhanced-Resolution Passive-Microwave EASE-Grid 2.0 Brightness Temperature Earth System Data Record, Remote Sensing, 10, 10.3390/rs10111793, 2018a.

Brown, R. D., and Derksen, C.: Is Eurasian October snow cover extent increasing?, Environmental Research Letters, 8, 10.1088/1748-9326/8/2/024006, 2013.

Chang, A., et al. : Nimbus-7 SMMR derived global snow cover parameters, Ann. Glaciol, 9, 39-44, 1987.

Che, T., et al. : Snow depth derived from passive microwave remote-sensing data in China, Annals of Glaciology, 49, 145-154, 2008.

Che, T., et al. : Estimation of snow depth from passive microwave brightness temperature data in forest regions of northeast China, Remote Sensing of Environment, 183, 334-349, 2016.

Chen, X., et al. : Developing a composite daily snow cover extent record over the Tibetan Plateau from 1981 to 2016 using multisource data, Remote Sensing of Environment, 215, 284-299, 10.1016/j.rse.2018.06.021, 2018.

Cheng, Z., et al. : Waste heat recovery from high-temperature solid granular materials: Energy challenges and opportunities, Renewable and Sustainable Energy Reviews, 116, 10.1016/j.rser.2019.109428, 2019.

Cohen, J., et al. : The Effect of Boreal Forest Canopy in Satellite Snow Mapping—A Multisensor Analysis, IEEE Transactions on Geoscience and Remote Sensing, 53, 6593-6607, 10.1109/tgrs.2015.2444422, 2015.

Colditz, R.: An Evaluation of Different Training Sample Allocation Schemes for Discrete and Continuous Land Cover Classification Using Decision Tree-Based Algorithms, Remote Sensing, 7, 9655-9681, 10.3390/rs70809655, 2015.

Coll, J., and Li, X.: Comprehensive accuracy assessment of MODIS daily snow cover products and gap filling methods, ISPRS Journal of Photogrammetry and Remote Sensing, 144, 435-452, 10.1016/j.isprsjprs.2018.08.004, 2018.

Czyzowska-Wisniewski, E. H., et al. : Fractional snow cover estimation in complex alpine-forested environments using an artificial neural network, Remote Sensing of Environment, 156, 403-417, 10.1016/j.rse.2014.09.026, 2015.

Dai, L., et al. : Snow depth and snow water equivalent estimation from AMSR-E data based on a priori snow characteristics in Xinjiang, China, Remote Sensing of Environment, 127, 14-29, 2012.

Dai, L., et al. : Evaluation of snow cover and snow depth on the Qinghai–Tibetan Plateau derived from passive microwave remote sensing, The Cryosphere, 11, 1933-1948, 10.5194/tc-11-1933-2017, 2017.

De Lannoy, G. J. M., et al. : Multiscale assimilation of Advanced Microwave Scanning Radiometer-EOS snow water equivalent and Moderate Resolution Imaging Spectroradiometer snow cover fraction observations in northern Colorado, Water Resources Research, 48, 10.1029/2011wr010588, 2012.

Derksen, C., et al. : Influence of sensor overpass time on passive microwave-derived snow cover parameters, Remote Sensing

of Environment, 71, 297-308, 2000.

Dietz, A. J., et al. : Remote sensing of snow – a review of available methods, International Journal of Remote Sensing, 33, 4094-4134, 10.1080/01431161.2011.640964, 2011.

Dobreva, I. D., and Klein, A. G.: Fractional snow cover mapping through artificial neural network analysis of MODIS surface reflectance, Remote Sensing of Environment, 115, 3355-3366, 10.1016/j.rse.2011.07.018, 2011.

Dong, C., and Menzel, L.: Producing cloud-free MODIS snow cover products with conditional probability interpolation and meteorological data, Remote Sensing of Environment, 186, 439-451, 10.1016/j.rse.2016.09.019, 2016.

Dong, C., and Menzel, L.: Snow process monitoring in montane forests with time-lapse photography, Hydrological Processes, 31, 2872-2886, 10.1002/hyp.11229, 2017a.

Dong, C., and Menzel, L.: Snow process monitoring in montane forests with a digital camera network, SnowHydro 2018 - International Conference on Snow Hydrology, Heidelberg, Germany, 2017b,

Dong, J., et al. : Using Air Temperature to Quantitatively Predict the MODIS Fractional Snow Cover Retrieval Errors over the Continental United States, Journal of Hydrometeorology, 15, 551-562, 10.1175/jhm-d-13-060.1, 2014.

Du, P., et al. : Random Forest and Rotation Forest for fully polarized SAR image classification using polarimetric and spatial features, ISPRS Journal of Photogrammetry and Remote Sensing, 105, 38-53, 10.1016/j.isprsjprs.2015.03.002, 2015.

Eibe Frank, M. A. H., and Ian H. Witten: The WEKA Workbench. Online Appendix for "Data Mining: Practical Machine Learning Tools and Techniques", Fourth ed., Morgan Kaufmann, 2016.

Flanner, M. G., et al. : Radiative forcing and albedo feedback from the Northern Hemisphere cryosphere between 1979 and 2008, Nature Geoscience, 4, 151-155, 10.1038/ngeo1062, 2011.

Frank, E., et al. : Data mining in bioinformatics using Weka, Bioinformatics, 20, 2479-2481, 2004.

Friedman, J. H.: Multivariate Adaptive Regression Splines, The Annals of Statistics, 19, 1-67, 1991.

Gafurov, A., and Bárdossy, A.: Cloud removal methodology from MODIS snow cover product, Hydrol. Earth Syst. Sci., 13, 1361-1373, 10.5194/hess-13-1361-2009, 2009.

Gao, J., et al. : Collapsing glaciers threaten Asia's water supplies, Nature, 19-21, 2019.

Gascoin, S., et al. : A snow cover climatology for the Pyrenees from MODIS snow products, Hydrology and Earth System Sciences, 19, 2337-2351, 10.5194/hess-19-2337-2015, 2015.

Gascoin, S., et al. : Theia Snow collection: high-resolution operational snow cover maps from Sentinel-2 and Landsat-8 data, Earth System Science Data, 11, 493-514, 10.5194/essd-11-493-2019, 2019.

Grippa, M., et al. : Siberia snow depth climatology derived from SSM/I data using a combined dynamic and static algorithm, Remote sensing of environment, 93, 30-41, 2004.

Grody, N. C., and Basist, A. N.: Global identification of snowcover using SSM/I measurements, IEEE Transactions on

geoscience and remote sensing, 34, 237-249, 1996.

Hall, D. K., et al. : Development of methods for mapping global snow cover using moderate resolution imaging spectroradiometer data, Remote Sensing of Environment, 54, 127-140, 1995.

Hall, D. K., et al. : Assessment of Snow-Cover Mapping Accuracy in a Variety of Vegetation-Cover Densities in Central Alaska, Remote Sensing of Environment, 66, 129-137, https://doi.org/10.1016/S0034-4257(98)00051-0, 1998.

Hall, D. K., et al. : Algorithm Theoretical Basis Document (ATBD) for the MODIS Snow and Sea Ice-Mapping Algorithms, 2001.

Hall, D. K., et al. : Assessment of the relative accuracy of hemispheric-scale snow-cover maps, Annals of Glaciology, 34, 24-30, 2002.

Hall, D. K., and Riggs, G. A.: Accuracy assessment of the MODIS snow products, Hydrological Processes, 21, 1534-1547, 10.1002/hyp.6715, 2007.

Han, M., et al. : An Algorithm Based on the Standard Deviation of Passive Microwave Brightness Temperatures for Monitoring Soil Surface Freeze/Thaw State on the Tibetan Plateau, IEEE Transactions on Geoscience and Remote Sensing, 53, 2775-2783, 10.1109/tgrs.2014.2364823, 2015.

Hao, S., et al. : Assessment of MODIS-Based Fractional Snow Cover Products Over the Tibetan Plateau, IEEE Journal of Selected Topics in Applied Earth Observations and Remote Sensing, 12, 533-548, 10.1109/jstars.2018.2879666, 2019.

Hao, X., et al. : Accuracy assessment of four cloud-free snow cover products over the Qinghai-Tibetan Plateau, International Journal of Digital Earth, 12, 375-393, 10.1080/17538947.2017.1421721, 2018.

Haykin, S. O.: Neural Networks and Learning Machines, 3 ed., Prentice Hall, 2009.

He, T., et al. : Analysis of global land surface albedo climatology and spatial-temporal variation during 1981-2010 from multiple satellite products, Journal of Geophysical Research: Atmospheres, 119, 10,281-210,298, 10.1002/2014jd021667, 2014.

Hecht-Nielsen, R.: Theory of the backpropagation neural network, in: Neural networks for perception, Elsevier, 65-93, 1992.

Henderson, G. R., et al. : Snow–atmosphere coupling in the Northern Hemisphere, Nature Climate Change, 8, 954-963, 10.1038/s41558-018-0295-6, 2018.

Hori, M., et al. : A 38-year (1978–2015) Northern Hemisphere daily snow cover extent product derived using consistent objective criteria from satellite-borne optical sensors, Remote Sensing of Environment, 191, 402-418, 10.1016/j.rse.2017.01.023, 2017.

Huang, X., et al. : Spatiotemporal dynamics of snow cover based on multi-source remote sensing data in China, The Cryosphere, 10, 2453-2463, 10.5194/tc-10-2453-2016, 2016.

Huang, Y., et al. : Improving MODIS snow products with a HMRF-based spatio-temporal modeling technique in the Upper

https://doi.org/10.5194/tc-2019-280
Preprint. Discussion started: 7 January 2020

Rio Grande Basin, Remote Sensing of Environment, 204, 568-582, 10.1016/j.rse.2017.10.001, 2018.

ARESLab: Adaptive Regression Splines toolbox for Matlab/Octave, 2016.

Jin, H., et al. : Assessing the impact of training sample selection on accuracy of an urban classification: a case study in Denver, Colorado, International Journal of Remote Sensing, 35, 2067-2081, 2014.

Josberger, E. G., and Mognard, N. M.: A passive microwave snow depth algorithm with a proxy for snow metamorphism, Hydrological Processes, 16, 1557-1568, 2002.

Kattenborn, T., et al. : UAV data as alternative to field sampling to map woody invasive species based on combined Sentinel-1 and Sentinel-2 data, Remote Sensing of Environment, 227, 61-73, 10.1016/j.rse.2019.03.025, 2019.

Kelly, R.: The AMSR-E snow depth algorithm: Description and initial results, Journal of The Remote Sensing Society of Japan, 29, 307-317, 2009.

Kim, R. S., et al. : Spectral analysis of airborne passive microwave measurements of alpine snowpack: Colorado, USA, Remote Sensing of Environment, 205, 469-484, 10.1016/j.rse.2017.07.025, 2018.

Kim, R. S., et al. : Estimating alpine snow depth by combining multifrequency passive radiance observations with ensemble snowpack modeling, Remote Sensing of Environment, 226, 1-15, 10.1016/j.rse.2019.03.016, 2019.

Kuter, S., et al. : Inversion of top of atmospheric reflectance values by conic multivariate adaptive regression splines, Inverse Problems in Science and Engineering, 23, 651-669, 10.1080/17415977.2014.933828, 2015.

Kuter, S., et al. : Retrieval of fractional snow covered area from MODIS data by multivariate adaptive regression splines, Remote Sensing of Environment, 205, 236-252, 10.1016/j.rse.2017.11.021, 2018.

Lemmetyinen, J., et al. : Retrieval of Effective Correlation Length and Snow Water Equivalent from Radar and Passive Microwave Measurements, Remote Sensing, 10, 10.3390/rs10020170, 2018.

Li, X., et al. : Snow Cover Identification with SSM/I Data in China, Journal of Applied Meteorological Science, 18, 12-20, 2007.

Liang, H., et al. : Fractional Snow-Cover Mapping Based on MODIS and UAV Data over the Tibetan Plateau, Remote Sensing, 9, 10.3390/rs9121332, 2017.

Liu, X., et al. : Assessment of Methods for Passive Microwave Snow Cover Mapping Using FY-3C/MWRI Data in China, Remote Sensing, 10, 10.3390/rs10040524, 2018.

Long, D. G., and Brodzik, M. J.: Optimum Image Formation for Spaceborne Microwave Radiometer Products, IEEE Transactions on Geoscience and Remote Sensing, 54, 2763-2779, 10.1109/TGRS.2015.2505677, 2016.

Luojus, K., et al. : Assessment of Seasonal snow Cover Mass in Northern Hemisphere During the Satellite-ERA, IGARSS 2018 - 2018 IEEE International Geoscience and Remote Sensing Symposium, 2018, 6255-6258, 2018.

Lyons, M. B., et al. : A comparison of resampling methods for remote sensing classification and accuracy assessment, Remote

Sensing of Environment, 208, 145-153, 10.1016/j.rse.2018.02.026, 2018.

Masson, T., et al. : An Assessment of Existing Methodologies to Retrieve Snow Cover Fraction from MODIS Data, Remote Sensing, 10, 10.3390/rs10040619, 2018.

Menne, M. J., et al. : An Overview of the Global Historical Climatology Network-Daily Database, Journal of Atmospheric and Oceanic Technology, 29, 897-910, 10.1175/jtech-d-11-00103.1, 2012b.

Metsämäki, S. J., et al. : A feasible method for fractional snow cover mapping in boreal zone based on a reflectance model, Remote Sensing of Environment, 95, 77-95, 10.1016/j.rse.2004.11.013, 2005.

Millard, K., and Richardson, M.: On the Importance of Training Data Sample Selection in Random Forest Image Classification: A Case Study in Peatland Ecosystem Mapping, Remote Sensing, 7, 8489-8515, 10.3390/rs70708489, 2015.

Moosavi, V., et al. : Fractional snow cover mapping from MODIS data using wavelet-artificial intelligence hybrid models, Journal of Hydrology, 511, 160-170, 10.1016/j.jhydrol.2014.01.015, 2014.

Mutanga, O., et al. : High density biomass estimation for wetland vegetation using WorldView-2 imagery and random forest regression algorithm, International Journal of Applied Earth Observation and Geoinformation, 18, 399-406, https://doi.org/10.1016/j.jag.2012.03.012, 2012.

Neale, C. M. U., et al. : Land-surface-type classification using microwave brightness temperatures from the Special Sensor Microwave/Imager, IEEE Transactions on Geoscience and Remote Sensing, 28, 829-838, 10.1109/36.58970, 1990.

Nguyen, L. H., et al. : Characterizing land cover/land use from multiple years of Landsat and MODIS time series: A novel approach using land surface phenology modeling and random forest classifier, Remote Sensing of Environment, 10.1016/j.rse.2018.12.016, 2018.

Pan, J., et al. : Wet snow detection in the south of China by passive microwave remote sensing, 2012 IEEE International Geoscience and Remote Sensing Symposium, 2012, 4863-4866, 2012.

Pan, M., et al. : Improving soil moisture retrievals from a physically-based radiative transfer model, Remote Sensing of Environment, 140, 130-140, 10.1016/j.rse.2013.08.020, 2014.

Parajka, J., and Blöschl, G.: Validation of MODIS snow cover images over Austria, Hydrol. Earth Syst. Sci., 10, 679-689, 10.5194/hess-10-679-2006, 2006.

Parajka, J., and Blöschl, G.: Spatio-temporal combination of MODIS images - potential for snow cover mapping, Water Resources Research, 44, 10.1029/2007wr006204, 2008.

Parajka, J., et al. : MODIS snow cover mapping accuracy in small mountain catchment – comparison between open and forest sites, Hydrology and Earth System Sciences Discussions, 9, 4073-4100, 10.5194/hessd-9-4073-2012, 2012.

Peng, G., et al. : A long-term and reproducible passive microwave sea ice concentration data record for climate studies and monitoring, Earth System Science Data, 5, 311-318, 10.5194/essd-5-311-2013, 2013.

Qu, Y., et al. : Rebuilding a Microwave Soil Moisture Product Using Random Forest Adopting AMSR-E/AMSR2 Brightness Temperature and SMAP over the Qinghai–Tibet Plateau, China, Remote Sensing, 11, 10.3390/rs11060683, 2019.

Quirós, E., et al. : Testing Multivariate Adaptive Regression Splines (MARS) as a Method of Land Cover Classification of TERRA-ASTER Satellite Images, Sensors, 9, 9011-9028, 10.3390/s91109011, 2009.

Revuelto, J., et al. : Topographic control of snowpack distribution in a small catchment in the central Spanish Pyrenees: intra- and inter-annual persistence, The Cryosphere, 2014.

Riggs, G. A., and Hall, D. K.: MODIS Snow Products Collection 6 User Guide, 2016.

Riggs, G. A., et al. : Overview of NASA's MODIS and Visible Infrared Imaging Radiometer Suite (VIIRS) snow-cover Earth System Data Records, Earth System Science Data, 9, 765-777, 10.5194/essd-9-765-2017, 2017.

Rodriguez-Galiano, V. F., et al. : An assessment of the effectiveness of a random forest classifier for land-cover classification, ISPRS Journal of Photogrammetry and Remote Sensing, 67, 93-104, https://doi.org/10.1016/j.isprsjprs.2011.11.002, 2012.

Romanov, P., and Tarpley, D.: Enhanced algorithm for estimating snow depth from geostationary satellites, Remote sensing of environment, 108, 97-110, 2007.

Rosenthal, W., and Dozier, J.: Automated Mapping of Montane Snow Cover at Subpixel Resolution from the Landsat Thematic Mapper, Water Resources Research, 32, 115-130, 10.1029/95WR02718, 1996.

Saberi, N.: Snow Properties Retrieval Using Passive Microwave Observations, Doctor of Philosophy, Geography Environmental Management, University of Waterloo, Waterloo, Ontario, Canada,, 156 pp., 2019.

Salomonson, V. V., and Appel, I.: Estimating fractional snow cover from MODIS using the normalized difference snow index, Remote Sensing of Environment, 89, 351-360, 10.1016/j.rse.2003.10.016, 2004.

Salomonson, V. V., and Appel, I.: Development of the Aqua MODIS NDSI fractional snow cover algorithm and validation results, IEEE Transactions on Geoscience and Remote Sensing, 44, 1747-1756, 10.1109/TGRS.2006.876029, 2006.

Savoie, M. H., et al. : Atmospheric corrections for improved satellite passive microwave snow cover retrievals over the Tibet Plateau, Remote Sensing of Environment, 113, 2661-2669, 2009.

Singh, P. R., and Gan, T. Y.: Retrieval of snow water equivalent using passive microwave brightness temperature data, Remote Sensing of Environment, 74, 275-286, 2000.

Smith, T., and Bookhagen, B.: Assessing uncertainty and sensor biases in passive microwave data across High Mountain Asia, Remote Sensing of Environment, 181, 174-185, 2016.

Sturm, M., et al. : Estimating snow water equivalent using snow depth data and climate classes, Journal of Hydrometeorology, 11, 1380-1394, 2010.

Sturm, M.: White water: Fifty years of snow research in WRR and the outlook for the future, Water Resources Research, 51, 4948-4965, 10.1002/2015wr017242, 2015.

https://doi.org/10.5194/tc-2019-280
Preprint. Discussion started: 7 January 2020

Sulla-Menashe, D., and Friedl, M. A.: Use Guide to collection 6 MODIS land cover (MCD12Q1 and MCD12C1), 2018.

Takala, M., et al. : Estimating northern hemisphere snow water equivalent for climate research through assimilation of space-borne radiometer data and ground-based measurements, Remote Sensing of Environment, 115, 3517-3529, 2011.

Tedesco, M., et al. : Artificial neural network-based techniques for the retrieval of SWE and snow depth from SSM/I data, Remote sensing of Environment, 90, 76-85, 2004.

Tedesco, M., and Jeyaratnam, J.: A New Operational Snow Retrieval Algorithm Applied to Historical AMSR-E Brightness Temperatures, Remote Sensing, 8, 2016.

Tran, H., et al. : A cloud-free MODIS snow cover dataset for the contiguous United States from 2000 to 2017, Sci. Data, 6, 180300, 10.1038/sdata.2018.300, 2019.

Tsai, et al. : Wet and Dry Snow Detection Using Sentinel-1 SAR Data for Mountainous Areas with a Machine Learning Technique, Remote Sensing, 11, 10.3390/rs11080895, 2019.

Wang, G., et al. : Fractional Snow Cover Mapping from FY-2 VISSR Imagery of China, Remote Sensing, 9, 10.3390/rs9100983, 2017.

Wang, X., et al. : Evaluation of MODIS snow cover and cloud mask and its application in Northern Xinjiang, China, Remote Sensing of Environment, 112, 1497-1513, 10.1016/j.rse.2007.05.016, 2008.

Wang, Y., et al. : AMSR2 snow depth downscaling algorithm based on a multifactor approach over the Tibetan Plateau, China, Remote Sensing of Environment, 231, 10.1016/j.rse.2019.111268, 2019.

Wiesmann, A., and Mätzler, C.: Microwave Emission Model of Layered Snowpacks, Remote Sensing of Environment, 70, 307-316, 1999.

Wolfe, R. E., et al. : Achieving sub-pixel geolocation accuracy in support of MODIS land science, Remote Sensing of Environment, 83, 31-49, https://doi.org/10.1016/S0034-4257(02)00085-8, 2002.

Xiao, X., et al. : Support vector regression snow-depth retrieval algorithm using passive microwave remote sensing data, Remote Sensing of Environment, 210, 48–64, 2018.

Xiao, X., et al. : Spatiotemporal variation of snow depth in the Northern Hemisphere from 1992 to 2016, The Cryosphere Discussions, 1-38, 10.5194/tc-2019-33, 2019.

Xin, Q., et al. : View angle effects on MODIS snow mapping in forests, Remote Sensing of Environment, 118, 50-59, 10.1016/j.rse.2011.10.029, 2012.

Xu, X., et al. : Global snow cover estimation with Microwave Brightness Temperature measurements and one-class in situ observations, Remote Sensing of Environment, 182, 227-251, 2016.

Yu, J., et al. : Developing Daily Cloud-Free Snow Composite Products From MODIS Terra–Aqua and IMS for the Tibetan Plateau, IEEE Transactions on Geoscience and Remote Sensing, 54, 2171-2180, 10.1109/tgrs.2015.2496950, 2016.

https://doi.org/10.5194/tc-2019-280
Preprint. Discussion started: 7 January 2020

Zhang, H., et al. : Ground-based evaluation of MODIS snow cover product V6 across China: Implications for the selection of NDSI threshold, Science of The Total Environment, 651, 2712-2726, 10.1016/j.scitotenv.2018.10.128, 2019.

Zhang, T.: Influence of the seasonal snow cover on the ground thermal regime: An overview, Reviews of Geophysics, 43, 589-590, 2005.

Zhang, T., et al. : Statistics and characteristics of permafrost and ground-ice distribution in the Northern Hemisphere, Polar Geography, 31, 47-68, 10.1080/10889370802175895, 2008.

Zhang, W., and Goh, A. T. C.: Multivariate adaptive regression splines and neural network models for prediction of pile drivability, Geoscience Frontiers, 7, 45-52, 10.1016/j.gsf.2014.10.003, 2016.

Zhao, W., et al. : Normalization of the temporal effect on the MODIS land surface temperature product using random forest regression, ISPRS Journal of Photogrammetry and Remote Sensing, 152, 109-118, 10.1016/j.isprsjprs.2019.04.008, 2019.

Zona, D., et al. : Cold season emissions dominate the Arctic tundra methane budget, Proceedings of the National Academy of Sciences, 113, 40-45, 10.1073/pnas.1516017113, 2016.

https://doi.org/10.5194/tc-2019-280
Preprint. Discussion started: 7 January 2020

List of Tables and Figures

Table 1. The input variables list. Line means this variable is not selected; asterisk indicated the variable is selected. The numbers in square brackets denote the number of variables. T19H is the brightness temperature (T) in 19-GHz channel with H polarization; T_19V_19H denotes the difference of brightness temperature between 19V and 19H channel; others are similar.

ID	Elements	Scenario-1 [18]	Scenario-2 [13]	Scenario-3 [3]	Scenario-4 [11]	Scenario-5 [12]	Scenario-6 [9]
1	Latitude	*	-	-	*	*	*
2	Longitude	*	-	-	*	*	-
3	DEM	*	-	-	*	*	-
4	Slope	*	-	-	*	*	-
5	Aspect	*	-	-	*	*	-
6	T19H	*	*	-	*	-	-
7	T19V	*	*	*	*	-	-
8	T37H	*	*	-	*	-	*
9	T37V	*	*	*	*	-	*
10	T91H	*	*	-	*	-	*
11	T91V	*	*	*	*	-	*
12	T_19V_19H	*	*	-	-	*	-
13	T_19V_37V	*	*	-	-	*	*
14	T_19H_37H	*	*	-	-	*	-
15	T_22V_19V	*	*	-	-	*	*
16	T_22V_91V	*	*	-	-	*	*
17	T_37V_37H	*	*	-	-	*	-
18	T_37V_91V	*	*	-	-	*	*
	References	(Liu et al., 2018)	(Xu et al., 2016)	(Kim et al., 2018)	(Xiao et al., 2018)		(Nguyen et al., 2018)

Table 2. The description of the revised Grody's algorithm. The unite is Kelvin (K).

Scattering Materials	Description
Scattering signature	$(Tb19V - Tb37V) > 0$ K
Precipitation	$(Tb22V \geq 259\ K)$ or $(254\ K \leq Tb22V \leq 258\ K\ and\ (Tb19V - Tb37V) \leq 2\ K)$
Clod desert	$(Tb19V - Tb19H) \geq 18\ K$ and $(Tb19V - Tb37V) \leq 10\ K$
Frozen ground	$(Tb19V - Tb19H) \geq 8\ K$ and $(Tb19V - Tb37V) \leq 2\ K$

https://doi.org/10.5194/tc-2019-280
Preprint. Discussion started: 7 January 2020

Table 3. Confusion matrix defining the accuracy of the predicted snow cover map reference to the in-situ snow cover observation. The characters (TP, FP, FN, TN) represent the number of records of snow-covered or snow-free in a particular conditions.

		Ground observation (true)	
		snow-covered (Positive)	snow-free (Negative)
Prediction	snow-covered (Positive)	TP (true positive)	FP (false positive)
	snow-free (Negative)	FN (false negative)	TN (true negative)
$OA = (TP + TN)/(TP + TN + FN + FP)$			
$OE = FN/(TP + FN)$			
$\mathrm{CE} = FP/(TP + FP)$			
$Pecision = TP/(TP + FP) = 1 - CE$			
$Recall = TP/(TP + FN) = 1 - OE$			
$Specificity = TN/(TN + FP)$			
$F1 = (2 * Precision * Recall)/(Precision + Recall)$			

Table 4. Variable selection tests in 6 scenarios on bare land type data for random forest method. The accuracy indexes of the estimation are calculated using OOB error estimates and 10-fold cross validation (CV).

	Indexes	Scenario-1	Scenario-2	Scenario-3	Scenario-4	Scenario-5	Scenario-6
OOB-error	R	0.776	0.679	0.590	0.778	0.774	0.708
	MAE	0.152	0.178	0.197	0.150	0.152	0.170
	RMSE	0.194	0.224	0.248	0.193	0.194	0.216
10-fold CV	R	0.777	0.682	0.596	0.778	0.775	0.710
	MAE	0.152	0.178	0.197	0.151	0.153	0.170
	RMSE	0.193	0.223	0.246	0.193	0.194	0.215
Time spent modeling / s		7.37	5.57	3.46	5.43	5.26	5.27

https://doi.org/10.5194/tc-2019-280
Preprint. Discussion started: 7 January 2020

Table 5. Performance of linear regression, ANN, MARS and random forest model using test datasets from 2010 for four land cover types. FSC indicate fractional snow cover. The number outside brackets indicate the number of pixels; The number inside brackets indicate their percentage.

Method	Land cover type	Time spent modeling/ s	R	MAE	RMSE	Max. /Min.	FSC < 0 (%)	FSC > 1 (%)
Linear regression	Forest	0.37	0.896	0.225	0.279	1.204 (-0.183)	44978 (10.21)	554 (0.13)
	Shrub	0.24	0.956	0.174	0.198	1.605/-0.382	335 (0.06)	125589 (24.17)
	Prairie	0.49	0.902	0.179	0.215	1.524 /-0.331	23604 (0.87)	632417 (23.22)
	Bare land	0.29	0.892	0.177	0.213	1.647 /-0.087	912 (0.10)	30208 (3.32)
ANN	Forest	51.09	0.895	0.315	0.401	0.949 / -0.520	161260 (36.62)	0 (0)
	Shrub	21.73	0.966	0.103	0.146	1.251 / -0.327	15267 (2.94)	38207 (7.35)
	Prairie	156.29	0.916	0.197	0.23	1.527 / -0.166	743 (0.03)	310285 (11.39)
	Bare land	35.31	0.932	0.174	0.203	1.730 / 0.173	0 (0)	39491 (4.34)
MARS	Forest	2518.10	0.838	0.208	0.254	2.132 / -0.122	8844 (2.01)	2823 (0.64)
	Shrub	1127.24	0.926	0.149	0.185	2.053 / -0.239	2977 (0.57)	121693 (23.42)
	Prairie	23406.76	0.912	0.164	0.197	1.764 / -0.733	4371 (0.16)	469416 (17.24)
	Bare land	2518.10	0.911	0.156	0.191	2.253 / -0.844	469 (0.05)	142155 (15.62)
Random Forest	Forest	52.16	0.916	0.202	0.245	0.960 / 0.011	0 (0)	0 (0)
	Shrub	16.76	0.975	0.118	0.162	0.999 /0.023	0 (0)	0 (0)
	Prairie	214.06	0.955	0.134	0.173	1.000 / 0.011	0 (0)	0 (0)
	Bare land	38.73	0.967	0.103	0.148	0.998 / 0.027	0 (0)	0 (0)

Table 6. The performance of random forest models on training and validation data under four land cover types.

Land cover type	Training			Validation		
	R	MAE	RMSE	R	MAE	RMSE
Forest	0.702	0.166	0.207	0.932	0.154	0.193
Shrub	0.772	0.146	0.191	0.971	0.142	0.199
Prairie	0.807	0.142	0.182	0.946	0.163	0.167
Bare land	0.807	0.144	0.190	0.950	0.152	0.198

https://doi.org/10.5194/tc-2019-280
Preprint. Discussion started: 7 January 2020

Table 7. The effect of precipitation, cold desert and frozen ground in snow cover misclassification. FP is false positive that means it is the number of pixels that are misclassified as snow cover by Random forest FSC. $SD_{obs} = 0$ denotes snow-free measured in station; $SC_{Grody} = 0$ denotes snow-free (precipitation, cold desert and frozen ground) determined by Grody's algorithm; $FSC > 0.3$ denotes snow cover by our method.

Land cover types	FP	$SC_{obs} = 0$ & $SC_{Grody} = 0$ & $FSC > 0.3$	Percentage
Overall	28638	20063	70.06%
Forest	1966	1528	77.72%
Shrub	519	485	93.45%
Prairie	13530	9554	70.61%
Bare land	12623	8496	67.31%

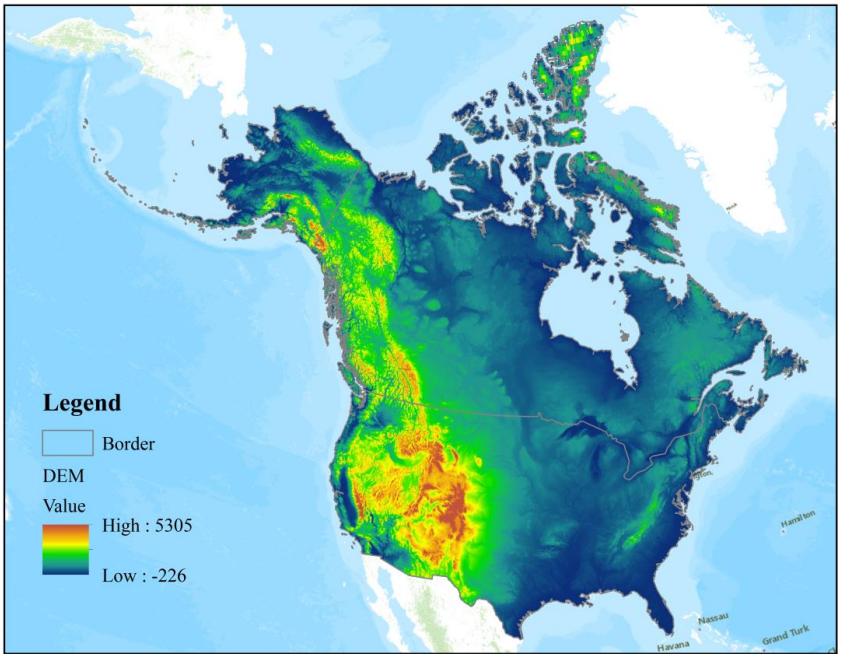

Fig. 1 Topographic map of North America.

https://doi.org/10.5194/tc-2019-280
Preprint. Discussion started: 7 January 2020

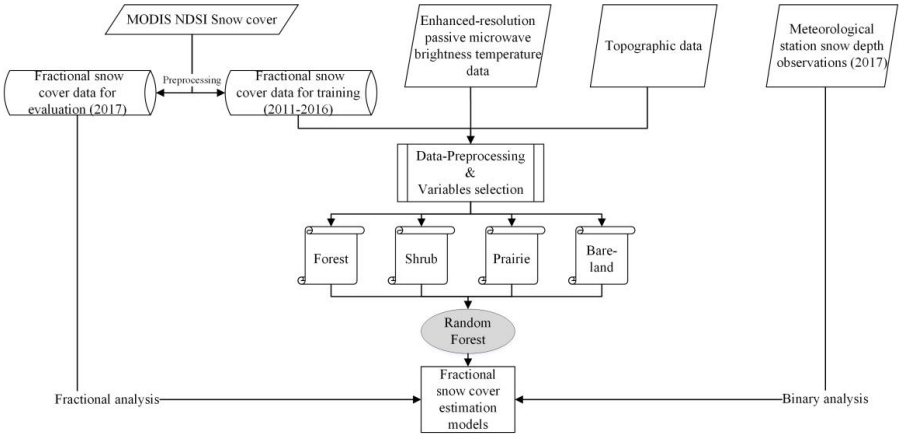

Fig. 2. Workflow diagram illustrating the processing of fractional snow cover retrieval.

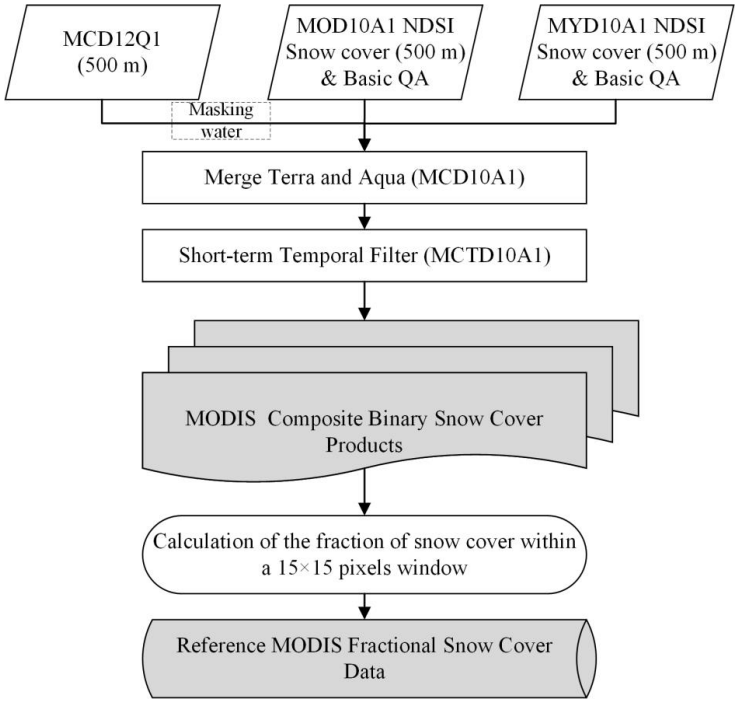

Fig. 3. The generation of MODIS fractional snow cover

https://doi.org/10.5194/tc-2019-280
Preprint. Discussion started: 7 January 2020

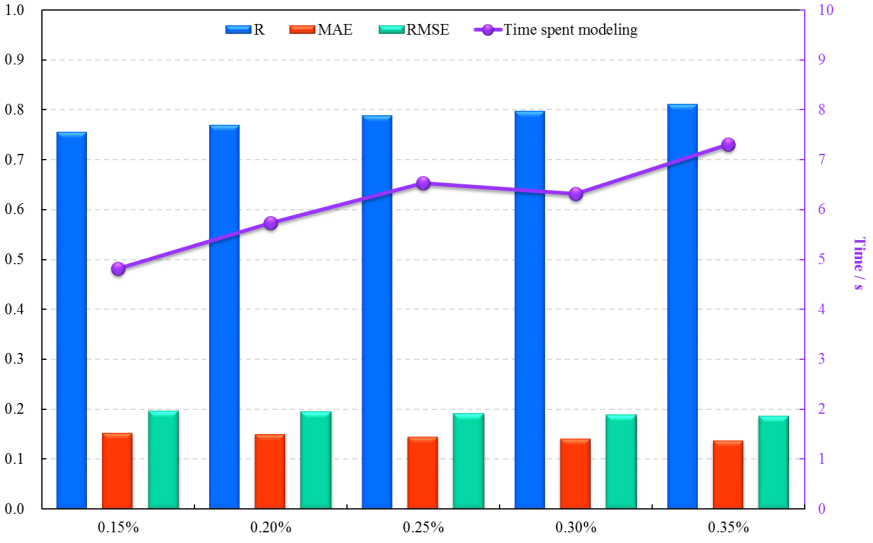

Fig. 4 Using OOB error estimates to evaluate the performance of random forest models with increasing training sample size for shrub type

Fig. 5. The variation of the accuracy indexes (MAE, RMSE and R) on four algorithms (linear regression, ANN, MARS and Random forest) for four land cover.

https://doi.org/10.5194/tc-2019-280
Preprint. Discussion started: 7 January 2020

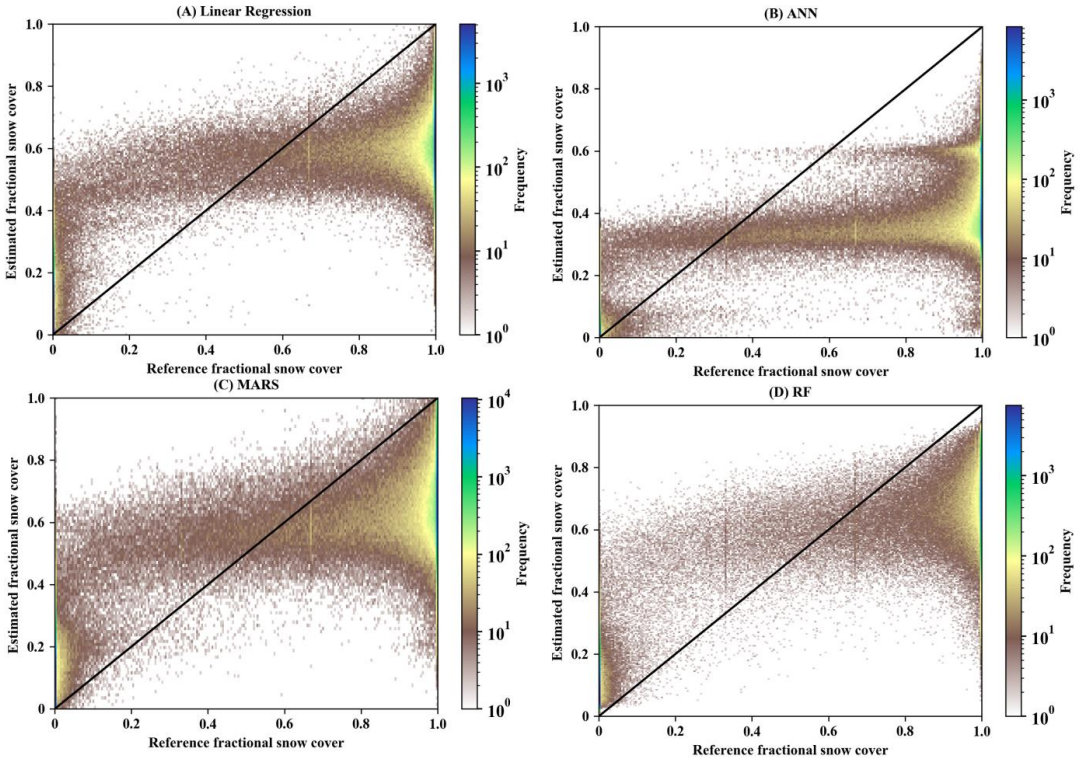

Fig. 6. The color-density scatter plots between the estimated fractional snow cover and MODIS-derived fractional snow cover for four algorithms (linear regression, ANN, MARS, and random forest) for forest type. The accuracy metric refer to Table 5. [Note: out-of-range fractional snow cover values of linear regression, ANN and MARS were truncated on 0 and 1]

5

https://doi.org/10.5194/tc-2019-280
Preprint. Discussion started: 7 January 2020

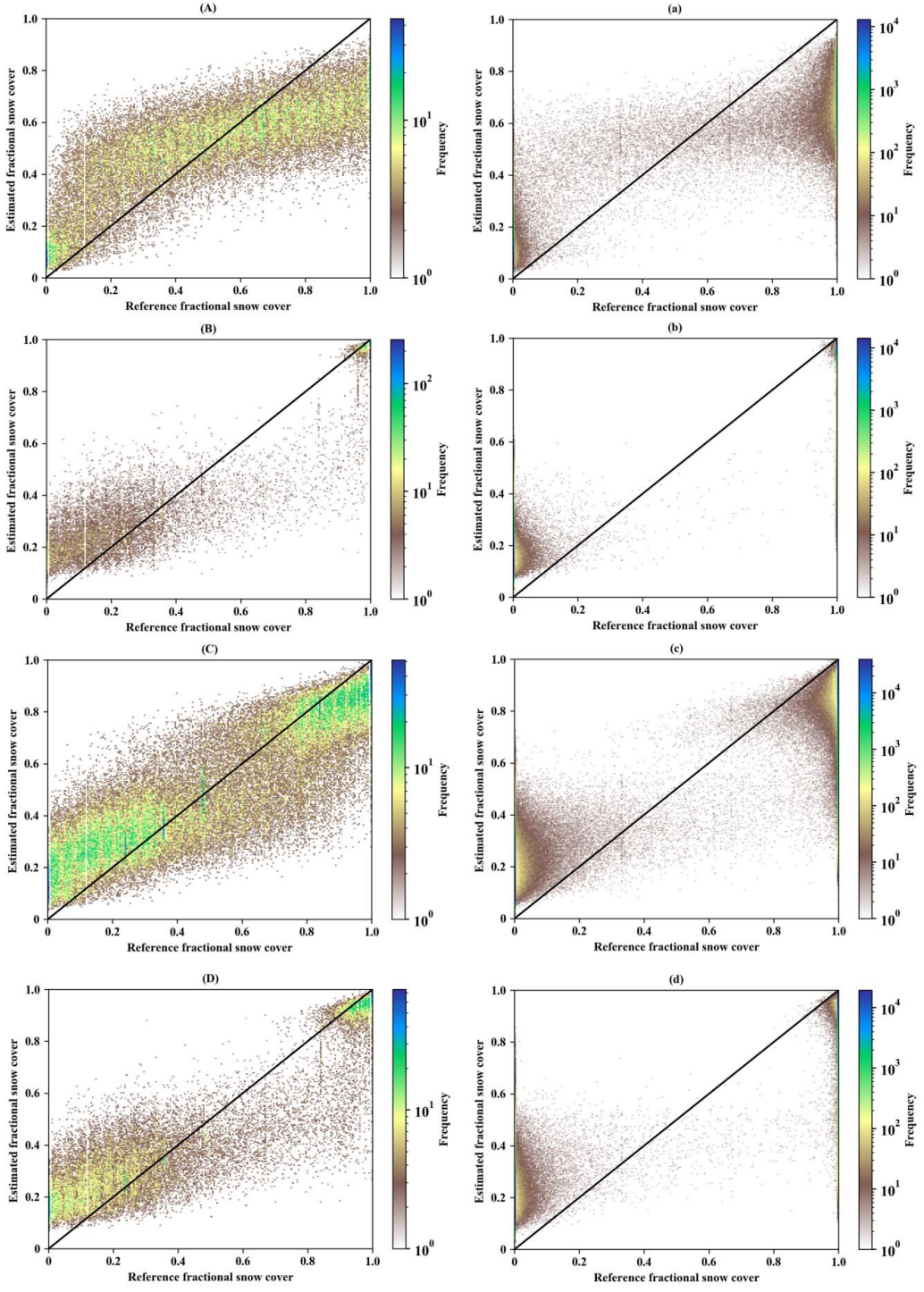

Fig. 7. The color-density scatter plots between the estimated fractional snow cover and MODIS-derived fractional snow cover for four land cover types (forest: A, a; shrub: B, b; prairie: C, c; bare land: D, d). Left column are the results in training stage (A-D); right column are the results in evaluation (a-d).

https://doi.org/10.5194/tc-2019-280
Preprint. Discussion started: 7 January 2020

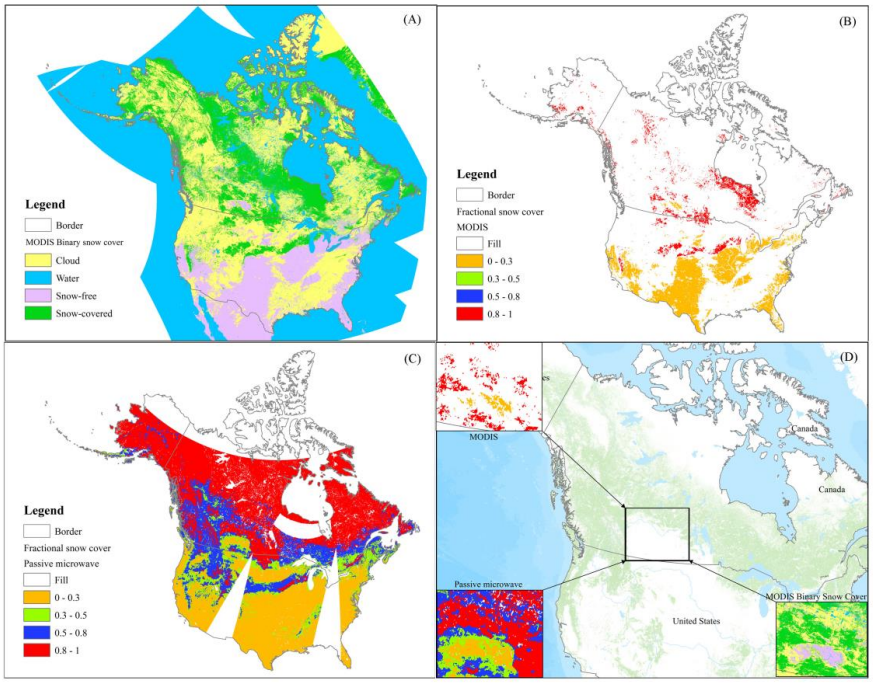

Fig. 8. Comparison of our estimated fractional snow cover (C, 6.25-km) with the reference MODIS fractional snow cover (B, 6.25-km) with respect to the MODIS composite binary snow cover products (A, 500-m) in the Central Canada area (D) on February 27th, 2017 (2017058). [Cf. the results in continuous value (Figure S-7 in the Appendix)]

5

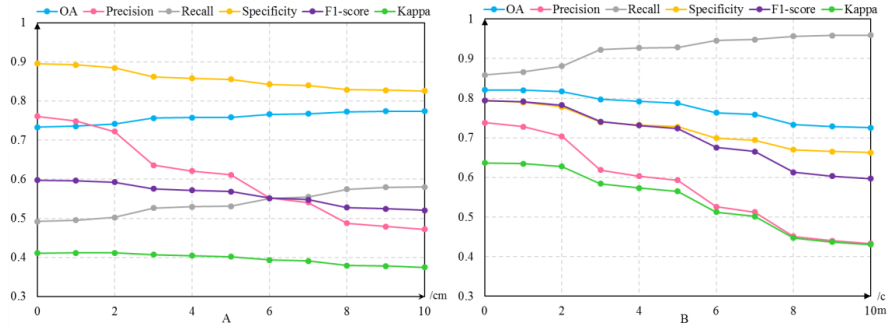

Fig. 9. The changes of accuracy indicators (OA, precision, recall, specificity, F1-score, kappa) for snow cover detection results of two algorithm (A: Grody' algorithm; B: Random forest) with increasing in situ snow depth value.

https://doi.org/10.5194/tc-2019-280
Preprint. Discussion started: 7 January 2020

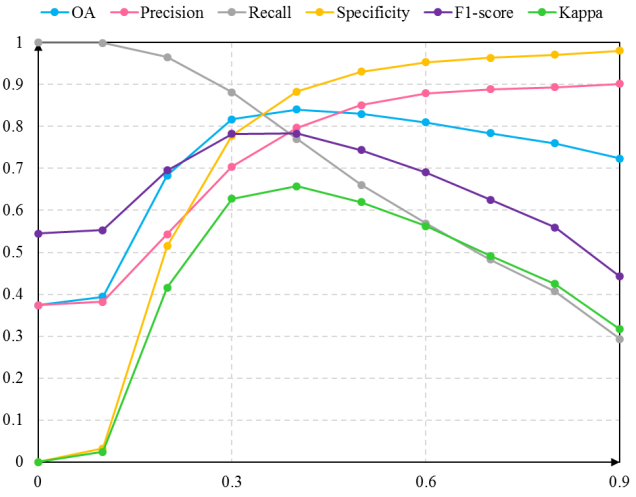

Fig. 10 The changes of accuracy indicators (OA, precision, recall, specificity, F1-score, kappa) for snow cover detection results with increasing fractional snow cover value (FSC).

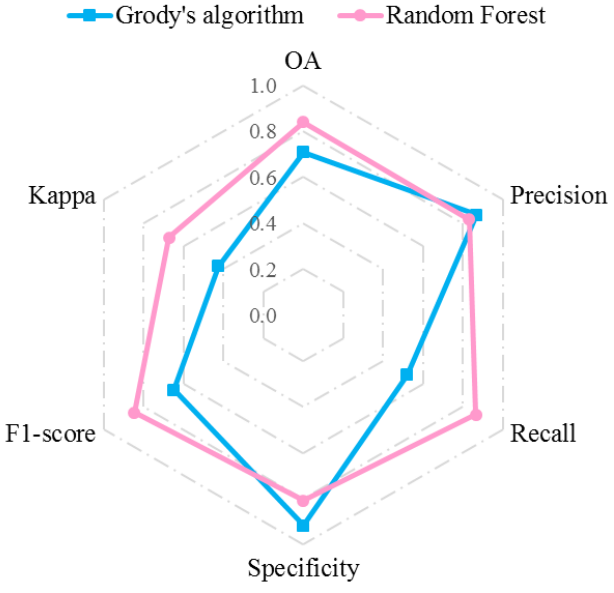

Fig. 11. The accuracy indicators (OA, precision, recall, specificity, F1-score, kappa) of snow cover detection from two algorithm (Grody' algorithm; Random forest).